NeuroImage 55 (2011) 1504–1518

Contents lists available at ScienceDirect

NeuroImage

journal homepage: www.elsevier.com/locate/ynimg

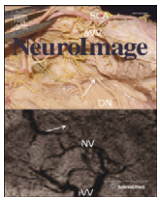

A new statistical test based on the wavelet cross-spectrum to detect time–frequency dependence between non-stationary signals: Application to the analysis of cortico-muscular interactions

Jérémie Bigot [a,b,*], Marieke Longcamp [c,e], Fabien Dal Maso [c], David Amarantini [c,d]

[a] Institut de Mathématiques de Toulouse et CNRS (UMR 5219), Université de Toulouse, France
[b] Center for Mathematical Modelling, Universidad de Chile, Chile
[c] LAPMA, Université de Toulouse, France
[d] Département de kinésiologie, Centre de réadaptation Marie-Enfant, Université de Montréal, Montreal, Quebec, Canada
[e] INCM (UMR 6193), CNRS-Université de la Méditerranée, Marseille, France

ARTICLE INFO

Article history:
Received 4 October 2010
Revised 7 December 2010
Accepted 12 January 2011
Available online 20 January 2011

Keywords:
Coherence
Cross-spectrum
Wavelet
Time–frequency dependence
Statistical testing
Cortico-muscular interactions

ABSTRACT

The study of the correlations that may exist between neurophysiological signals is at the heart of modern techniques for data analysis in neuroscience. Wavelet coherence is a popular method to construct a time–frequency map that can be used to analyze the time–frequency correlations between two time series. Coherence is a normalized measure of dependence, for which it is possible to construct confidence intervals, and that is commonly considered as being more interpretable than the wavelet cross-spectrum (WCS). In this paper, we provide empirical and theoretical arguments to show that a significant level of wavelet coherence does not necessarily correspond to a significant level of dependence between random signals, especially when the number of trials is small. In such cases, we demonstrate that the WCS is a much better measure of statistical dependence, and a new statistical test to detect significant values of the cross-spectrum is proposed. This test clearly outperforms the limitations of coherence analysis while still allowing a consistent estimation of the time–frequency correlations between two non-stationary stochastic processes. Simulated data are used to investigate the advantages of this new approach over coherence analysis. The method is also applied to experimental data sets to analyze the time–frequency correlations that may exist between electroencephalogram (EEG) and surface electromyogram (EMG).

Introduction

In the last decades, the oscillatory behavior of neurophysiological signals has drawn increased attention among neuroscientists Buzsaki and Draguhn (2004), Salenius and Hari (2003), Schnitzler and Gross (2005), Varela et al. (2001). In this framework, the correlations occurring at different frequencies between two or more signals are assumed to indicate oscillatory coupling of neuronal groups. Typically, neurophysiological signals contain noise at different frequency bands and are thus considered as random time series or stochastic processes. Fourier analysis has been widely used for studying the spectral contents of such signals, and the correlations that may exist at different frequencies between electroencephalogram (EEG), electromyogram (EMG) and magnetoencephalogram (MEG) Grosse et al. (2002), Halliday et al. (1995, 1998), Mima and Hallett (1999b), Mima et al. (2000) have been investigated using Fourier coherence. If the investigated signals are assumed to be stationary, then estimates of the auto and cross-spectra can be calculated to compute an estimation of the coherence at different frequencies. However, signals typically encountered in biomedical applications are non-stationary times series whose frequency behavior changes with time. A powerful alternative to Fourier analysis is the wavelet transform which is a widely developed tool for the study of non-stationary signals as it allows a simultaneous analysis of the content of a signal over time and frequency (see e.g. Mallat (1998) for an introduction to wavelet analysis, and Allen and MacKinnon (2010) for a review and comparison of time–frequency methods for the analysis of EEG signals). In recent years, wavelet coherence has been proposed as an alternative to Fourier coherence for the analysis of time–frequency dependence between two time series. There exists a rich literature on estimating time–frequency dependence between time series using localized transforms, see e.g. Ombao et al. (2001), Sanderson et al. (2010), Whitcher et al. (2005), Whitcher (2000). Applications of time–frequency coherence can be found in neuroscience Lachaux et al. (2002), Ombao and Van Bellegem (2008), Zhan et al. (2006), but also in geophysics Grinsted et al. (2004), Maraun and Kurths (2004), and wind engineering Gurley et al. (2003) to name but a few. The wavelet coherence is a normalized measure (between 0 and 1) of

* Corresponding author.
E-mail address: jeremie.bigot@math.univ-toulouse.fr (J. Bigot).

1053-8119/$ – see front matter © 2011 Elsevier Inc. All rights reserved.
doi:10.1016/j.neuroimage.2011.01.033

time–frequency dependence between two time series that is commonly considered as being more interpretable than the wavelet cross-spectrum (WCS). Statistical tests have been proposed in Gish and Cochran (1988), Halliday et al. (1995), Maris et al. (2007) to derive confidence intervals for the Fourier coherence between two time series. A similar statistical test, based on averaging over repeated trials, has been suggested in Zhan et al. (2006) to determine if the time–frequency coherence between neurophysiological signals is significant or not.

The objective of this paper is to discuss the relevance of wavelet coherence as a statistical measure of time–frequency dependence between random time series, and to compare it to the statistical information contained in the WCS. The main contributions are the following: first theoretical and empirical arguments are detailed to show some limitations of wavelet coherence analysis. In particular, we exhibit some drawbacks of the test proposed in Zhan et al. (2006) which may yield an erroneous estimation of time–frequency correlations between two signals.

Second, as an alternative to the limitations of wavelet coherence, a new statistical test to detect significant values of the WCS is proposed. Contrary to the standard test in Gish and Cochran (1988), Halliday et al. (1995), Zhan et al. (2006) to derive confidence intervals for the coherence, our test correctly estimates the areas in the time–frequency plane where the dependence between the time series is truly significant, and does not detect any area where no correlation between the signals exists (an example being the case of two independent Gaussian time series with zero mean). The idea of the test is rather simple. High values of the WCS should correspond to areas in the time–frequency plane where there exists a correlation between the time series. Thus, we first derive a threshold such that, with high probability and under the null hypothesis that the observed signals are independent Gaussian times series, all the values of the WCS fall below this threshold. This means that the values of the WCS that do not correspond to a significant level of time–frequency dependence lie below a certain value with large probability. We show that this probabilistic bound is a threshold that can be easily computed from the data. A standard criticism on the use of the cross-spectrum is that one cannot assess the strength of dependence because this measure does not take into account the variances of the time series contrary to the coherence. To overcome this issue, our method automatically includes an estimation of the variance of the two time series in the computation of the threshold. Therefore, the procedure is fully data-driven, and it is in particular adapted to the case where one pair of time series has a higher magnitude of covariance than the second pair. This new test is also based on averaging over repeated trials as in Zhan et al. (2006). However, the proposed probabilistic bound is non-asymptotic, meaning that it holds for any values of the number of trials and length of the signals. Moreover, the test is valid for any Gaussian processes with zero-mean without assuming stationarity or making parametric assumptions on the covariance functions of the time series. It is therefore very robust in the sense that excellent results can be obtained for a broad class of random signals using very few trials.

Third, a detailed simulation study is proposed to investigate the advantages of this new approach over coherence analysis, and the method is applied to experimental data sets to analyze the time–frequency correlations that may exist between EEG and EMG signals.

Methods

The standard test for detecting significant values of wavelet coherence

First, let us fix the notations and recall the definitions of wavelet transform, WCS and wavelet coherence between stochastic processes. Let $\mathbf{x} = [x(t_k)]_{k=1}^{T}$ and $\mathbf{y} = [y(t_k)]_{k=1}^{T}$ denote two random time series of length T observed at regularly spaced time points t_k. The wavelet transform (WT) of $\mathbf{x}$ (resp. $\mathbf{y}$) at scale $s>0$ and time u is defined as (see e.g. Mallat (1998))

$$W_{\mathbf{x}}(s,u) = \sum_{k=1}^{T} x(t_k)\overline{\psi_{s,u}(t_k)}$$

where $\bar{z}$ denotes the conjugate of a complex number z,

$$\psi_{s,u}(t_k) = \frac{1}{\sqrt{s}}\psi\left(\frac{t_k-u}{s}\right),$$

and $\psi(\cdot)$ is an oscillating function called wavelet which should satisfy a number of regularity and admissibility conditions (see e.g. Mallat (1998)). The WT can be seen as a time–frequency representation of a signal by converting the scale parameter s to a frequency parameter ω. This correspondence depends on a specific frequency ω_0, which represents the central frequency location of the energy ψ in the Fourier domain, and the relationship between frequency and scale is given by $\omega \approx \frac{\omega_0}{s}$. Thus the WT at frequency ω and time u can be expressed as

$$W_{\mathbf{x}}(\omega,u) = \sum_{k=1}^{T} x(t_k)\sqrt{\frac{\omega}{\omega_0}}\,\psi\left(\frac{\omega}{\omega_0}(t_k-u)\right).$$

A commonly used wavelet in practice is the Morlet wavelet, which is a complex-valued function, defined as

$$\psi(u) = \pi^{-1/4} e^{i\omega_0 u} e^{-u^2/2}, \tag{2.1}$$

where ω_0 is the central frequency of ψ. A Morlet wavelet is thus a complex sine wave within a Gaussian envelope, and the parameter ω_0 determines the number of oscillations of the wavelet within this envelope. In all the numerical experiments presented in this paper, we took $\omega_0 = 7$ as it is a common choice in wavelet analysis of neurophysiological signals, see e.g. Tallon-Baudry et al. (1996).

The wavelet coherence at frequency ω and time u between the time series $\mathbf{x}$ and $\mathbf{y}$ is then defined by (see e.g. Grinsted et al. (2004), Maraun and Kurths (2004), Zhan et al. (2006))

$$R^2_{\mathbf{xy}}(\omega,u) = \frac{|S_{\mathbf{xy}}(\omega,u)|^2}{S_{\mathbf{x}}(\omega,u)S_{\mathbf{y}}(\omega,u)},$$

where $S_{\mathbf{xy}}(\omega,u)$ is the WCS between $\mathbf{x}$ and $\mathbf{y}$, and $S_{\mathbf{x}}(\omega,u)$ (resp. $S_{\mathbf{y}}(\omega,u)$) is the wavelet auto-spectrum (WAS) of $\mathbf{x}$ (resp. $\mathbf{y}$) defined respectively as

$$S_{\mathbf{xy}}(\omega,u) = \mathbb{E}\left(W_{\mathbf{x}}(\omega,u)\overline{W_{\mathbf{y}}(\omega,u)}\right) \text{ and } S_{\mathbf{x}}(\omega,u) = \mathbb{E}|W_{\mathbf{x}}(\omega,u)|^2,$$

where $\mathbb{EZ}$ denotes the expectation of a random variable Z.

Recall that if one observes n independent realizations Z_m, $m=1,\ldots,n$ of Z then $\mathbb{E}Z = lim_{n\to+\infty}\frac{1}{n}\sum_{m=1}^{n} Z_m$ by the law of large numbers. Hence, if one observes data consisting of n repeated trials $(\mathbf{x}_m)_{m=1,\ldots,n} = \left([x_m(t_k)]_{k=1}^{T}\right)_{m=1,\ldots,n}$ and $(\mathbf{y}_m)_{m=1,\ldots,n} = \left([y_m(t_k)]_{k=1}^{T}\right)_{m=1,\ldots,n}$ (viewed as n independent realizations of the stochastic processes $\mathbf{x}$ and $\mathbf{y}$, respectively) then the WCS between the two time series is naturally estimated by the following empirical wavelet cross-spectrum

$$\hat{S}_{\mathbf{xy}}(\omega,u) = \frac{1}{n}\sum_{m=1}^{n} W_{\mathbf{x}_m}(\omega,u)\overline{W_{\mathbf{y}_m}(\omega,u)}$$

and an estimator of the wavelet coherence is given by the following empirical wavelet coherence

$$\hat{R}^2_{\mathbf{xy}}(\omega,u)=\frac{\left|\sum_{m=1}^{n} W_{\mathbf{x}_m}(\omega,u)\overline{W_{\mathbf{y}_m}(\omega,u)}\right|^2}{\left(\sum_{m=1}^{n}|W_{\mathbf{x}_m}(\omega,u)|^2\right)\left(\sum_{m=1}^{n}|W_{\mathbf{y}_m}(\omega,u)|^2\right)}.$$

Note that the "true" coherence $R^2_{\mathbf{xy}}(\omega,u)$ is the limit as the number of trials tends to infinity ($n\to+\infty$) of the above empirical coherence $\hat{R}^2_{\mathbf{xy}}(\omega,u)$.

The wavelet coherence is a normalized measure (between 0 and 1) of time–frequency dependence between two time series. Note that if $\mathbf{x}$ and $\mathbf{y}$ are independent zero-mean processes then, at any frequency ω and time u, one has that

$$S_{\mathbf{xy}}(\omega,u)=\mathbb{E}(W_{\mathbf{x}}(\omega,u))\mathbb{E}\left(\overline{W_{\mathbf{y}}(\omega,u)}\right)=0$$

and thus $R^2_{\mathbf{xy}}(\omega,u)=0$. To the contrary, if there exists a linear relationship $W_{\mathbf{y}}(\omega,u)=aW_x(\omega,u)$ between $\mathbf{x}$ and $\mathbf{y}$ at some frequency ω and time u with $a\neq 0$, then $S_{\mathbf{xy}}(\omega,u)=\bar{a}S_{\mathbf{x}}(\omega,u)$ and $S_{\mathbf{y}}(\omega,u)=|a|^2S_{\mathbf{x}}(\omega,u)$ which implies that $R^2_{\mathbf{xy}}(\omega,u)=1$. Therefore, values of wavelet coherence close to 1 are interpreted as evidence for a significant time–frequency correlation between $\mathbf{x}$ and $\mathbf{y}$. In practice, as a preliminary step, the observed times series can be centered to have zero mean over the n repetitions before computing the empirical wavelet cross-spectrum and coherence.

To derive a threshold to detect automatically significant values of the coherence, most authors in the literature use a procedure proposed in Gish and Cochran (1988) to test the null hypothesis H_0 that the two time series $\mathbf{x}$ and $\mathbf{y}$ are independent Gaussian white noise. Based on repeated observations $(\mathbf{x}_m,\mathbf{y}_m)_{m=1,\dots,n}$ with $n\geq 2$, it has been shown in Gish and Cochran (1988) that, under H_0, $\hat{R}^2_{\mathbf{xy}}(\omega,u)\leq r_\alpha$ with probability $1-\alpha$ where the threshold r_α is equal to

$$r_\alpha=1-\alpha^{1/(n-1)}\ \text{ for } 0\leq\alpha\leq 1.$$

Therefore, at level $\alpha=5\%$, a detection threshold is $r_\alpha=1-0.05^{1/(n-1)}$ and values of $\hat{R}^2_{\mathbf{xy}}(\omega,u)$ that are above this level are considered as a significant level of coherence.

A new statistical test for detecting significant values of the wavelet cross-spectrum

It is often argued that wavelet coherence is more interpretable than the WCS which is a non-normalized measure of dependence. Indeed, at first glance, it seems difficult to judge if an observed value of the cross-spectrum is significant. Let us recall that the standard method to detect significant values of the coherence is based on a statistical procedure to test the null hypothesis H_0 that the components $x(t_k)$ and $y(t_k)$ of the two time series $\mathbf{x}$ and $\mathbf{y}$ are independent and identically distributed (iid) centered Gaussian variables (that is $x(t_k)\sim_{\text{iid}}N(0,\sigma_x^2)$ and $y(t_k)\sim_{\text{iid}}N(0,\sigma_y^2)$ for $k=1,\dots,T$). We propose to derive a new statistical procedure to test the more general null hypothesis $H_0(\Sigma_x,\Sigma_y)$ that the random time series $\mathbf{x}=[x(t_k)]_{k=1}^T$ and $\mathbf{y}=[y(t_k)]_{k=1}^T$ of length T are independent Gaussian vectors with zero mean and covariance matrix Σ_x and Σ_y respectively, namely

$$H_0\left(\Sigma_x,\Sigma_y\right):\mathbf{x}\text{ and }\mathbf{y}\text{ are independent vectors of length T with }\mathbf{x}\sim N(0,\Sigma_x)\text{and }\mathbf{y}\sim N\left(0,\Sigma_y\right),$$

where $N(0,\Sigma)$ denotes a Gaussian random vector of length T with zero mean and covariance matrix Σ. Note that $H_0(\Sigma_x,\Sigma_y)$ includes the case where the components of the two time series $\mathbf{x}$ and $\mathbf{y}$ are iid centered Gaussian variables with variance σ_x^2 and σ_y^2 which corresponds to the choice $\Sigma_x=\sigma_x^2I_T$ and $\Sigma_y=\sigma_y^2I_T$ where I_T denotes the identity matrix of size $T\times T$.

Theoretical arguments developed in the Appendix show that under $H_0(\Sigma_x,\Sigma_y)$, $|\hat{S}_{\mathbf{xy}}(\omega,u)|\leq\hat{\lambda}_\alpha$ with probability larger than $1-\alpha$ where the threshold $\hat{\lambda}_\alpha$ is equal to

$$\hat{\lambda}_\alpha=\frac{\hat{\rho}_x\,\hat{\rho}_y}{\left(1+\sqrt{\frac{T}{n}}\right)^2}\left(-\frac{log(\alpha/2)}{n}+\sqrt{-\frac{2log(\alpha/2)}{n}}\right),$$

with $\hat{\rho}_x^2$ (resp. $\hat{\rho}_y^2$) being the largest eigenvalue of the empirical covariance matrix of the time series $\mathbf{x}$ (resp. $\mathbf{y}$). We refer the Appendix for a precise definition, and for the computation of $\hat{\lambda}_\alpha$ in practice. Using such a procedure, the values of the empirical cross-spectrum that are lower than the threshold $\hat{\lambda}_\alpha$ (with e.g. $\alpha=5\%$) are considered as not significant, whereas the values $|\hat{S}_{\mathbf{xy}}(\omega,u)|$ that are above the threshold $\hat{\lambda}_\alpha$ can be considered as being a truly significant level of time–frequency dependence at frequency ω and time u. Note that this test does not make any parametric assumption on the covariance matrices Σ_x and Σ_y.

As explained previously, coherence is a normalized measure of dependence that is usually considered as being more interpretable than the cross-spectrum which does not take into account the variance of the time series to assess the strength of dependence. Hence, if one pair of time series has a very large auto-spectrum this may cause the cross-spectrum to be very large even in the absence of dependence between two time series. In the computation of the threshold $\hat{\lambda}_\alpha$, the term $\frac{\hat{\rho}_x\,\hat{\rho}_y}{\left(1+\sqrt{\frac{T}{n}}\right)^2}$ corresponds to a data-based upper bound of the amplitude of the auto-spectra of the time series.

Indeed, consider first the null hypothesis $H_0(\sigma_x^2I_T,\ \sigma_y^2I_T)$. Under such an assumption, the test is based on the properties that

- with probability larger than $1-\alpha$: $\left|\hat{S}_{\mathbf{xy}}(\omega,u)\right|^2\leq\sigma_x^2\sigma_y^2\ *C(n,\alpha)$ where $C(n,\alpha)=\left(-\frac{log(\alpha/2)}{n}+\sqrt{-\frac{2log(\alpha/2)}{n}}\right)^2$ is a constant depending only on n and the level of the test α.
- with large probability: $\hat{\lambda}_\alpha^2\approx\sigma_x^2\sigma_y^2\ *C(n,\alpha)$.

Hence, the computation of the threshold $\hat{\lambda}_\alpha$ includes an estimation of the variance σ_x^2 and σ_y^2 of each time series.

In the more general case where $\Sigma_x\neq\sigma_x^2I_T$ or $\Sigma_y\neq\sigma_y^2I_T$, the test uses the properties that

- with probability larger than $1-\alpha$: $\left|\hat{S}_{\mathbf{xy}}(\omega,u)\right|^2\leq S_{\mathbf{x}}(\omega,u)S_{\mathbf{y}}(\omega,u)*C(n,\alpha)$ where $S_{\mathbf{x}}(\omega,u)$ (resp. $S_{\mathbf{y}}(\omega,u)$) is the wavelet auto-spectrum of $\mathbf{x}$ (resp. $\mathbf{y}$).
- with large probability: $\hat{\lambda}_\alpha^2\geq S_{\mathbf{x}}(\omega,u)S_{\mathbf{y}}(\omega,u)*C(n,\alpha)$, which corresponds to a data-based upper bound for the product of the wavelet auto-spectra of the two time series.

Thus, the above arguments show that the test automatically adapts to the case where one pair of time series has a large wavelet auto-spectra (which results in a large wavelet cross-spectrum) while still controlling the level of dependence between the two time series. Such a test is also non-asymptotic in the sense that it holds for any value of number of trials n and length of the signals T.

Results

Simulated data

Let us first consider some simulated examples to illustrate the differences between the test based on wavelet coherence (using the threshold r_α), and the test based on the WCS (using the data-based

threshold $\hat{\lambda}_\alpha$) for the detection of time–frequency correlations between random signals.

Analysis of time–frequency dependent Gaussian processes

Example 1. We simulate n independent realizations (trials) of the following two Gaussian times series with zero mean of length T = 1000 ms generated with sampling rate 1 kHz:

$$x(t_k) = Z(sin(2\pi\omega_1 t_k)\mathbb{1}_{[0,u_1[}(t_k) + sin(2\pi\omega_2 t_k)\mathbb{1}_{[u_1,u_2[}\left(t_k\right)\Big) + \sigma_x\epsilon_{1,k}$$
$$y(t_k) = Z(a_1 sin(2\pi\omega_1 t_k)\mathbb{1}_{[0,u_1]}(t_k) + a_2 sin(2\pi\omega_2 t_k)\mathbb{1}_{[u_1,u_2[}\left(t_k\right)\Big) + \sigma_y\epsilon_{2,k}, \quad (3.1)$$

where Z ~ N (0,1), with $t_k = 1,\ldots,T$, $\omega_1 = 10Hz$, $\omega_2 = 30Hz$, $u_1 = 300$ ms, $u_2 = 700$ ms, $a_1 = 1.2$, $a_2 = 1.5$, and where the $\epsilon_{,k}$'s are independent Gaussian variables with zero mean and variance 1. The parameters σ_x, σ_y are levels of noise that can be adjusted according to the desired signal-to-noise ratio (SNR). For two reals a and b, $\mathbb{1}_{[a,b[}(t_k)$ denotes the function which is equal to 0 if $t_k < a$ or $t_k \geq b$ and to 1 otherwise. Note that for the signal $\mathbf{x}$, the SNR is defined as $20log_{10}(1/\sigma_x)$, and for the signal $\mathbf{y}$, the SNR is $20log_{10}(a_2/\sigma_y)$. The two times series are thus two sine waves with random amplitude of different frequency and time localization with additive Gaussian white noise. It should be noted that the amplitude of the two time series are correlated on the time intervals [0, 300 ms] and [300 ms, 700 ms] at frequency $\omega_1 = 10Hz$ and $\omega_2 = 30Hz$ respectively. Thus $\mathbf{x}$ and $\mathbf{y}$ are time–frequency dependent Gaussian processes.

An example of realization for each time series with a SNR equal to −5 dB is given in Fig. 1(a). The wavelet coherence $R^2_{\mathbf{xy}}(\omega,u)$ and the "true" WCS $S_{\mathbf{xy}}(\omega,u)$ are displayed in Fig. 1(d, e). The empirical coherence $\hat{R}^2_{\mathbf{xy}}(\omega,u)$ computed with $n = 10$ trials is displayed in Fig. 2 (c) together with a time–frequency map showing (in red) the values of the empirical coherence that are above the threshold r_α with $\alpha = 5\%$.

First, remark the wavelet coherence $R^2_{\mathbf{xy}}(\omega,u)$ and the "true" WCS $S_{\mathbf{xy}}(\omega,u)$ do not contain the same information. Large value of the cross-spectrum are mainly observed in narrow frequency bands centered at the frequencies $\omega = 10Hz$ and $\omega = 30Hz$ and on the time intervals [0, 300] ms and [300, 700] ms which is consistent with model (2). To the contrary, the large values of wavelet coherence are much more spread in the time–frequency plane, and are found for example around the point $(\omega, u) = 20$ Hz, 300 ms which is somewhat unexpected in the sense that there does not exist such a time–frequency correlation between the two time series in model (3.1).

Secondly, it can be seen from Fig. 2(d) that the statistical test using the threshold r_α finds significant values for the coherence in the time–frequency plane around the points $(\omega, u) = 10$ Hz, 200 ms and $(a, u) =$ 30 Hz, 500 ms which is consistent with model (3.1) used to simulate the data. However, the test also detects areas in the time–frequency plane which do not correspond to significant values of the true coherence displayed in Fig. 1(d), or to an expected time–frequency dependence for such data. Now, let us consider the new statistical test suggested in Section 2.2 that is based on the thresholding of the empirical WCS with the data-based threshold $\hat{\lambda}_\alpha$. In Fig. 2(f) we display the result of this thresholding procedure for data from model (3.1), i.e., Example 1 with $n = 10$ trials. One can see that the results are much better than those obtained by thresholding the empirical wavelet coherence with r_α. This new test correctly estimates the areas in the time–frequency plane where the dependence between the time series is truly significant, and does not detect any area where no correlation between the signals exists.

Results obtained using only $n = 2$ trials are displayed in Fig. 3. It can be seen that the results using the threshold r_α to detect significant values of the wavelet coherence are worse. Indeed, most of the truly significant values of the coherence found previously with $n = 10$ trials (around the points $(\omega,u) = (10Hz, 200ms)$ and $(\omega,u) = (30Hz, 500ms)$) fall below the threshold r_α when using $n = 2$ trials. To the contrary, the results displayed in Fig. 3(f) show that our procedure using the threshold $\hat{\lambda}_\alpha$ to detect significant values of the wavelet cross-spectrum performs very well with only $n = 2$ trials.

Coherence detection in the absence of time–frequency dependence between signals

Let us now compare the behavior of the two tests when there is a priori no time–frequency dependence between the signals. A simple example being the case of two independent Gaussian time series with zero mean. For this consider the following simulated experiments:

Example 2. We simulate n independent realizations (trials) of the following two times series of length T = 1000 ms generated with sampling rate 1 kHz:

$$x(t_k) = Z(sin(2\pi\omega_1 t_k)\mathbb{1}_{[0,u_1[}(t_k) + sin(2\pi\omega_2 t_k)\mathbb{1}_{[u_1,u_2[}(t_k)) + \sigma_x\epsilon_{1,k}$$
$$y(t_k) = \sigma_y\epsilon_{2,k}, \quad (3.2)$$

where $Z \sim N(0,1)$, with $t_k = 1,\ldots,T$, $\omega_1 = 10$ Hz, $\omega_2 = 30$ Hz, $u_1 = 300$ ms, $u_2 = 700$ ms, and where the $\epsilon_{j,\,k}$'s are independent Gaussian variables with zero mean and variance $\mathbb{1}$. The second signal $\mathbf{y}$ is therefore a purely Gaussian white noise (we took $\sigma_y = \sigma_x$ in this numerical example), and therefore the coherence between $\mathbf{x}$ and $\mathbf{y}$ is expected to be zero. An example of coherence estimation using model (3.2) with $n = 10$ is given in Fig. 4. It can be seen that the test finds many significant values for the wavelet coherence which is clearly not consistent with the data from model (3.2). Consider now the results of our test on Examples 2. One can see from Fig. 4 that all the values of the empirical WCS fall below the data-based threshold $\hat{\lambda}_\alpha$. Therefore, contrary to the test based on the empirical wavelet coherence, our test does not find significant values for the WCS which is consistent with model (3.2).

Example 3. Let us simulate again n independent realizations (trials) $(\mathbf{x}_m)_{m=1,\ldots,n}$ and $(\mathbf{y}_m)_{m=1,\ldots,n}$ of the two times series $\mathbf{x}$ and $\mathbf{y}$ from model (3.1) with a SNR equal to $-5dB$. Then, we apply data shuffling to the trials from the second time series to artificially create independence across samples. More precisely, we propose to compare the detection of time–frequency dependence when computing the wavelet coherence and the WCS either from the raw data $(\mathbf{x}_m)_{m=1,\ldots,n}$ and $(\mathbf{y}_m)_{m=1,\ldots,n}$ or from the shuffled trials $(\mathbf{x}_m)_{m=1,\ldots,n}$ and $(\tilde{\mathbf{y}}_m)_{m=1,\ldots,n}$ where $\tilde{\mathbf{y}}_m = \mathbf{y}_{m+1}$ (see Fig. 5 for an example with $n = 30$). By data shuffling, the time series $\mathbf{x}_m$ and $\mathbf{y}_m$ are independent samples, and it is thus expected there is no coherence between such signals. It can be seen in Fig. 5(f) that the test on coherence detection finds many significant values for the wavelet coherence using the shuffled data which is clearly not satisfactory. To the contrary, Fig. 5 (h) shows that our procedure does not find significant values for the WCS when using the shuffled data while still performing a consistent estimation of the WCS when using the raw data, see Fig. 5(d). When the number of trials is small (see Fig. 6(h) with $n = 10$), the results of the data shuffling show remaining significant values of the WCS which are due to large values of the auto-spectrum of $\mathbf{x}$ and $\mathbf{y}$, but with much smaller areas than without data shuffling, see Fig. 6(d).

Robustness to Gaussianity

The derivation of the threshold $\hat{\lambda}_\alpha$ relies on the assumption that the time series are Gaussian processes. Therefore, one may wonder if the test is robust to such an hypothesis.

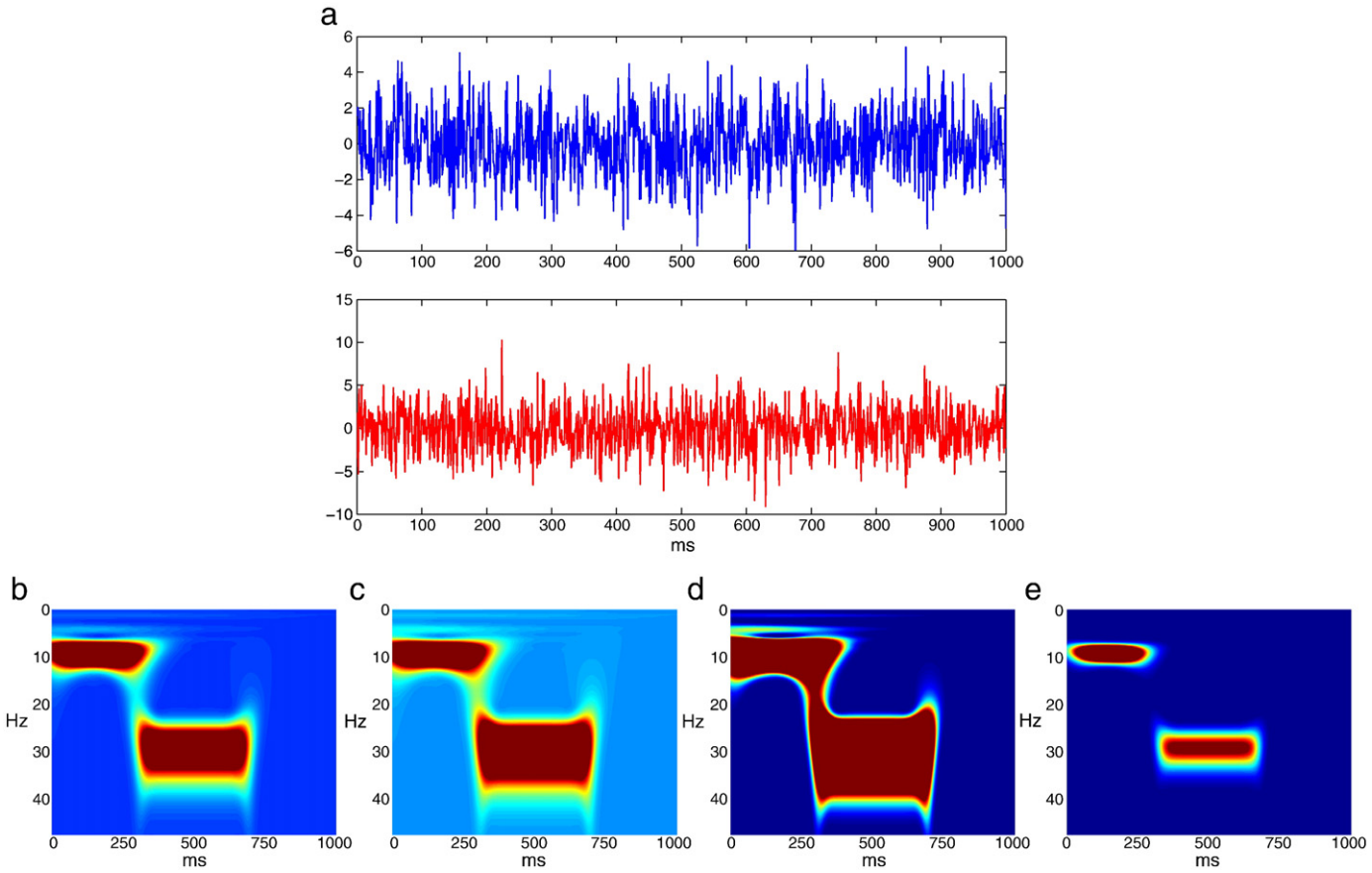

Fig. 1. Example 1 (a) An example of time series $\mathbf{x}_1$ and $\mathbf{y}_1$ generated from model (3.1) with SNR $= -5dB$. (b) Wavelet auto-spectrum $S_{\mathbf{x}}(\omega,u)$. (c) Wavelet auto-spectum $S_{\mathbf{y}}(\omega,u)$. (d) Wavelet coherence $R^2_{\mathbf{xy}}(\omega,u)$. (e) Wavelet cross-spectrum $|S_{\mathbf{xy}}(\omega,u)|^2$. The two time series have a common sine wave of 10 Hz from 1 ms to 300 ms and another common sine wave of 30Hz from 300 ms to 700 ms in each trial.

Example 4. To study robustness to Gaussianity, we simulate n independent realizations (trials) of the following times series of length $T=1000$ ms with sampling rate 1 kHz.

$$x(t_k) = Z(sin(2\pi\omega_1 t_k)\mathbb{1}_{[0,u_1[}(t_k) + sin(2\pi\omega_2 t_k)\mathbb{1}_{[u_1,u_2[}(t_k)) + \sigma_x\epsilon_{1,k}$$

$$y(t_k) = Z(a_1 sin(2\pi\omega_1 t_k)\mathbb{1}_{[0,u_1[}(t_k) + a_2 sin(2\pi\omega_2 t_k)\mathbb{1}_{[u_1,u_2[}(t_k)) + \sigma_y\epsilon_{2,k}, \quad (3.3)$$

where Z~Laplace (0,1) and $\epsilon_{1,k}$~iid Laplace (0,1) $\epsilon_{2,k}$~iid Laplace (0,1) with $u_1,u_2,\omega_1,\omega_2,a_1,a_2$, σ_x, σ_y chosen as in model (3.1), and where Laplace (0,1) denotes a random variable following a Laplace distribution with zero mean and variance one. The time series in model (3.3) thus follows a Laplace distribution, and are such that they have the same wavelet coherence and WCS than the Gaussian time series from model (3.1) which are displayed in Fig. 1(d, e).

An example of realization from model (3.3) with a SNR equal to -5 dB is displayed in Fig. 7(a). It can be seen that time series following such a Laplace distribution are signals which contains isolated peaks. Hence, when compared to the Gaussian signals from model (3.1) in Fig. 1(a), they are more appropriate to model spiky processes. The results of our testing procedure displayed in Fig. 7(g) are very satisfactory. The test correctly estimates the areas in the time–frequency plane where the dependence between the time series is truly significant. Moreover, it does not detect any area where no correlation between the signals exists. Again, the results using the standard test to detect significant values of the wavelet coherence are not so satisfactory, see Fig. 7(e).

Evaluation of type I and type II errors: effects of n and SNR

To test the performances of this new procedure to detect significant values of time–frequency dependence between random signals, we propose to generate time series from model (3.1) using different values for the SNR and the number of trials, and to compare the results with those given by the standard test in Gish and Cochran (1988); Zhan et al. (2006) to detect significant values of wavelet coherence. Recall that the quality of a statistical test is expressed in terms of its type I and type II error rate. The type I error rate is the probability of a false positive, rejecting the null hypothesis at frequency-time point (w,u) when it is true. The type II error rate is the probability of a false negative i.e. accepting the null hypothesis at frequency-time point (w,u) when there is a truly significant level of time–frequency dependence at (ω,u) between the two-time series. The goal of this simulation study is to evaluate the type I and type II errors of the two tests at various points (w,u)in the time–frequency plane.

The different values for the factors in the simulations are SNR $=-10$, -20 dB and $n=10$, 100 trials. For each combination of these two factors, we compare the two tests on $M=100$ repetitions from model (3.1). For $m=1,\ldots M$, each repetition m consists in simulating n trials from model (3.1) for a given level of SNR. Then, based on these n trials, one constructs two time–frequency testing maps $T_m(\omega,u)$ (one for each test) containing the result of each statistical test with $T_m(\omega,u)=0$ if the test accepts the null hypothesis H_0, and $T_m(\omega,u)=1$ if the test rejects H_0. For some repetition m, it is possible that the two (or only one) tests perform poorly or very good. It is therefore important to quantify the behavior of such tests on average, and not to draw conclusions from a single set of n trials.

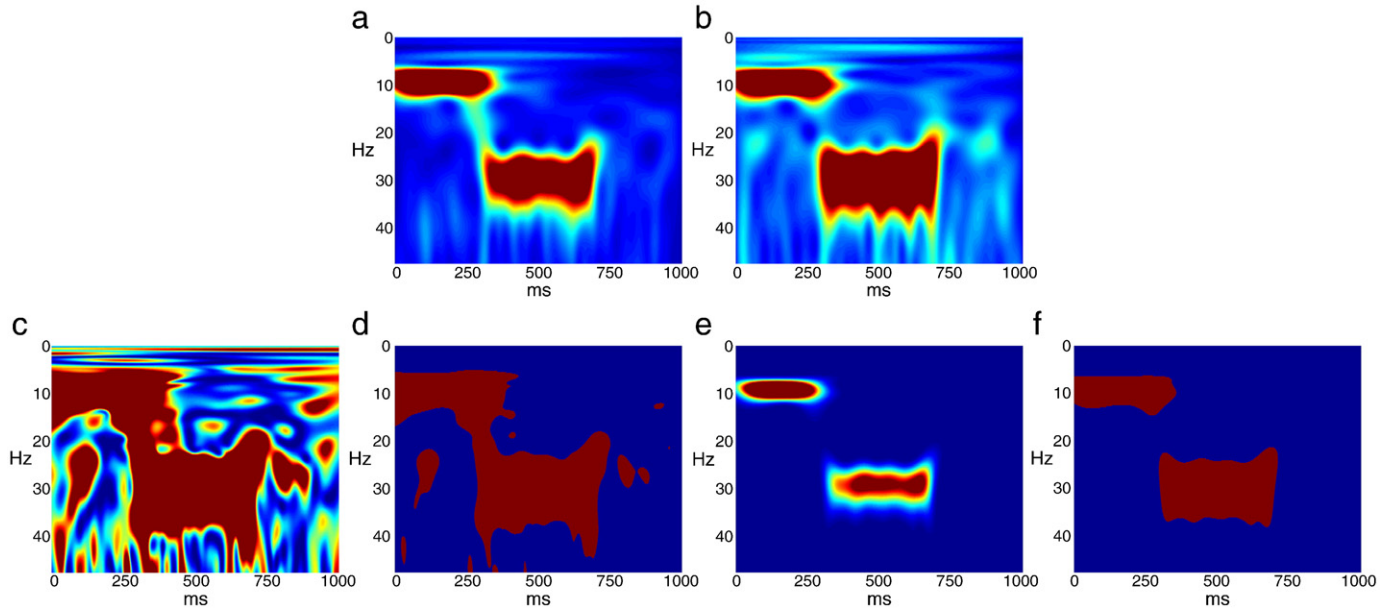

Fig. 2. Example 1—Automatic detection of time–frequency dependence using $n=10$ trials with SNR $=-5dB$. (a) Empirical wavelet auto-spectum $\hat{S}_{\mathbf{x}}(\omega,u)$. (b) Empirical wavelet auto-spectum $\hat{S}_{\mathbf{y}}(\omega,u)$. (c) Empirical wavelet coherence $\hat{R}^2_{\mathbf{xy}}(\omega,u)$. (d) Significant values (in red) of the empirical wavelet coherence that are above the threshold r_α. (e) Empirical WCS $|\hat{S}_{\mathbf{xy}}(\omega,u)|^2$. (f) Significant values (in red) of the empirical WCS that are above the threshold $\hat{\lambda}_\alpha$. The value of α is 5% for both thresholds.

For this purpose, the performances of each test, over the $M=100$ repetitions, can be visualized from the following averaged time–frequency testing map:

$$\overline{T}(\omega,u)=\frac{1}{M}\sum_{m=1}^{M} T_m(\omega,u).$$

Note that $\overline{T}(\omega,u)$ is a value between 0 and 1 that can be interpreted as the probability that the test rejects the null hypothesis H_0 at frequency-time point (w,u). Values close to 1 indicate that (on average) the test rejects H_0 at frequency ω and time u, while values close to 0 indicate that (on average) the test accepts H_0. Therefore, comparing the values $\overline{T}(\omega,u)$ to the true WCS and the true wavelet coherence is way to evaluate the type I and type II errors of each test. Results are displayed in Figs. 8 and 9, and the main comments that can be made are the following:

- as the SNR decreases the time–frequency maps given by the true wavelet coherence $R^2_{\mathbf{xy}}(\omega,u)$ and the true WCS $|S_{\mathbf{xy}}(\omega,u)|^2$ are more and more similar, compare Figs. 1(a), (b) with Figs. 8, 9(a), (d).
- the number of false positives using our test is extremely low. This means that a value of the empirical WCS that is above the threshold $\hat{\lambda}_\alpha$ can be considered as being a truly significant level of

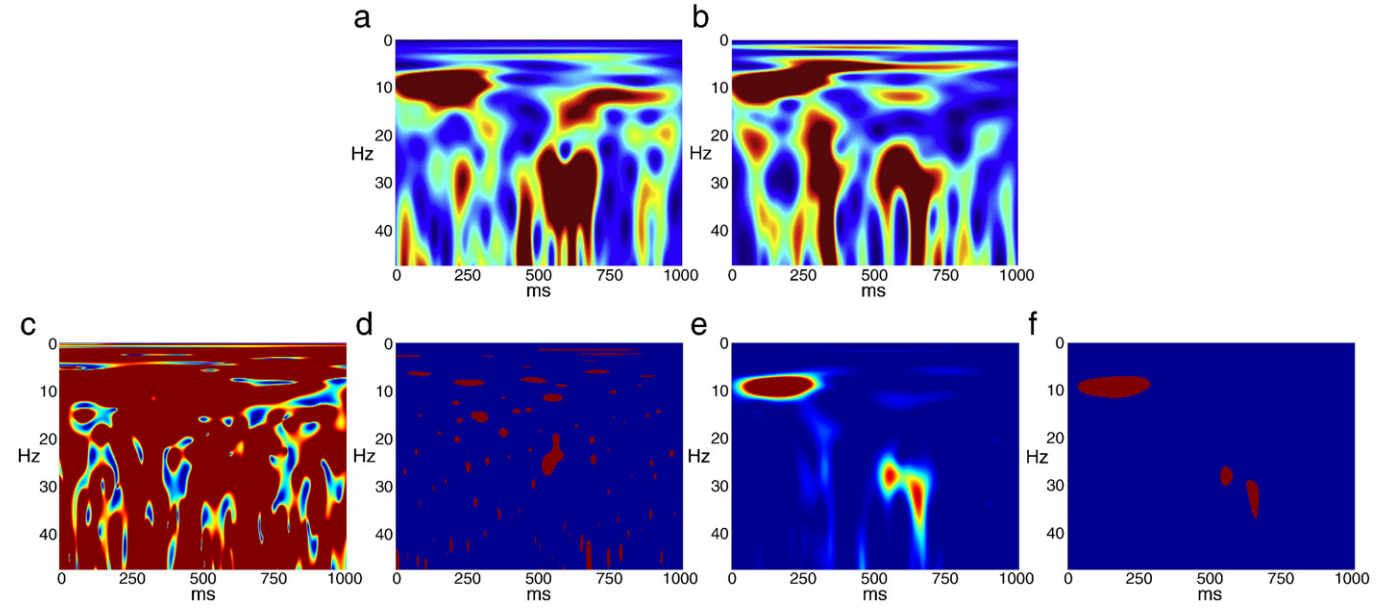

Fig. 3. Example 1—Automatic detection of time–frequency dependence using $n=2$ trials with SNR $=-5dB$. (a) Empirical wavelet auto-spectum $\hat{S}_{\mathbf{x}}(\omega,u)$. (b) Empirical wavelet auto-spectum $\hat{S}_{\mathbf{y}}(\omega,u)$. (c) Empirical wavelet coherence $\hat{R}^2_{\mathbf{xy}}(\omega,u)$. (d) Significant values (in red) of the empirical wavelet coherence that are above the threshold r_α. (e) Empirical WCS $|\hat{S}_{\mathbf{xy}}(\omega,u)|^2$. (f) Significant values (in red) of the empirical WCS that are above the threshold $\hat{\lambda}_\alpha$ - The value of α is 5% for both thresholds.

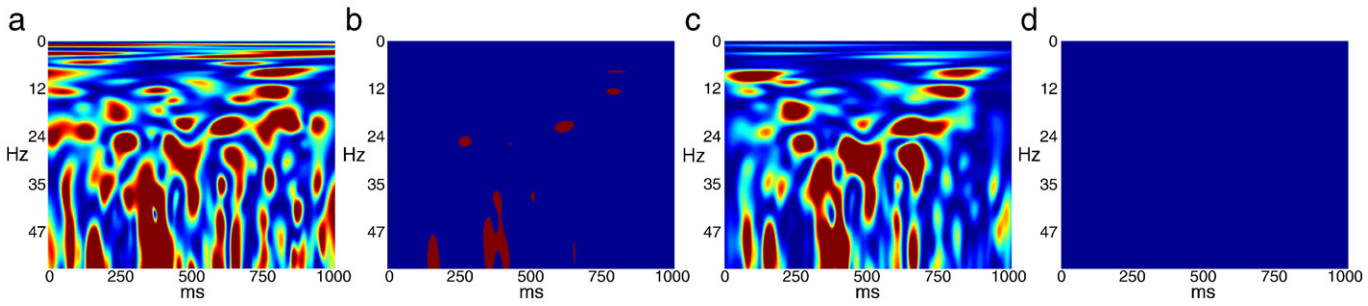

Fig. 4. Example 2—Automatic detection of time–frequency dependence using $n = 10$ trials with SNR $= -10dB$. (a) Empirical wavelet coherence $\hat{R}^2_{\mathbf{xy}}(\omega, u)$. (b) Significant values (in red) of the empirical wavelet coherence that are above the threshold r_α. (c) Empirical WCS $|\hat{S}_{\mathbf{xy}}(\omega, u)|^2$. (d) No significant values are found for the empirical WCS using the threshold $\hat{\lambda}_\alpha$. The value of α is 5% for both thresholds.

time–frequency dependence with a high confidence. To the contrary, the test on empirical wavelet coherence using the threshold r_α yields many false positive.

— when the signal-to-noise ratio is high (SNR $= -10$ db), our test performs very well with few trials ($n = 10$). For a higher SNR, the performances of our test are still very satisfactory when using more trials.

Application to the analysis of corticomuscular interactions

To assess the usefulness of the proposed approach with an experimental example, we compare the results of the two tests when applied to neurophysiological signals. Data were collected from a single healthy adult male volunteer, as part of a study on the effects of force level on corticomuscular interactions during submaximal voluntary isometric contractions. The participant was secured in a seated position with the right knee 60° flexed on a calibrated dynamometer (System 4 Pro, Biodex Medical Systems, Shirley, NY, USA) used to record the net joint torque around the knee at 1000 Hz. He was asked to perform blocks of isometric contractions of the right knee extensors at either 10% or 20% of previously determined maximal voluntary contraction (MVC), in a randomized order. Each contraction level was performed 10 times per block for 6 seconds, and was followed by a 6-second rest interval. Each block was followed by 3 minutes of rest, and overall, 10 blocks were performed leading to a total of 100 contractions per MVC level. The required MVC level was controlled through a visual torque feedback displayed on a screen placed 1 m in front of the participant. The participant had to exert the required torque level as soon as torque feedback was provided, and to maintain it as accurately as possible through the duration of the contraction until disappearance of the torque feedback. During the contractions, he was required to keep its upper body and left lower limb muscles relaxed and its arms rested on each tight.

Electroencephalographic signal (EEG) was recorded reference-free at 1024 Hz using a 64-channel ActiveTwo system (BioSemi, Amsterdam, Netherlands; electrode impedances below 5 k), with electrodes arranged according to the International 10-20 system. The continuous EEG signal was high-pass filtered at 0.5 Hz (zero-lag, 4th order Butterworth filter) and referenced to the FCz electrode. The Cz electrode was selected for further analysis as the electrode optimally located to record cerebral activity directly linked to right lower limb muscles contraction Masakado and Nielsen (2008); Perez et al. (2006). Following suitable skin preparation Hermens et al. (2000), surface electromyographic signal (EMG) was recorded from Vastus Medialis (VM) at 1000 Hz using a Bagnoli-8 system (DE-2.1, Delsys, Inc., Boston, MA, USA) with the reference electrode on the left radial

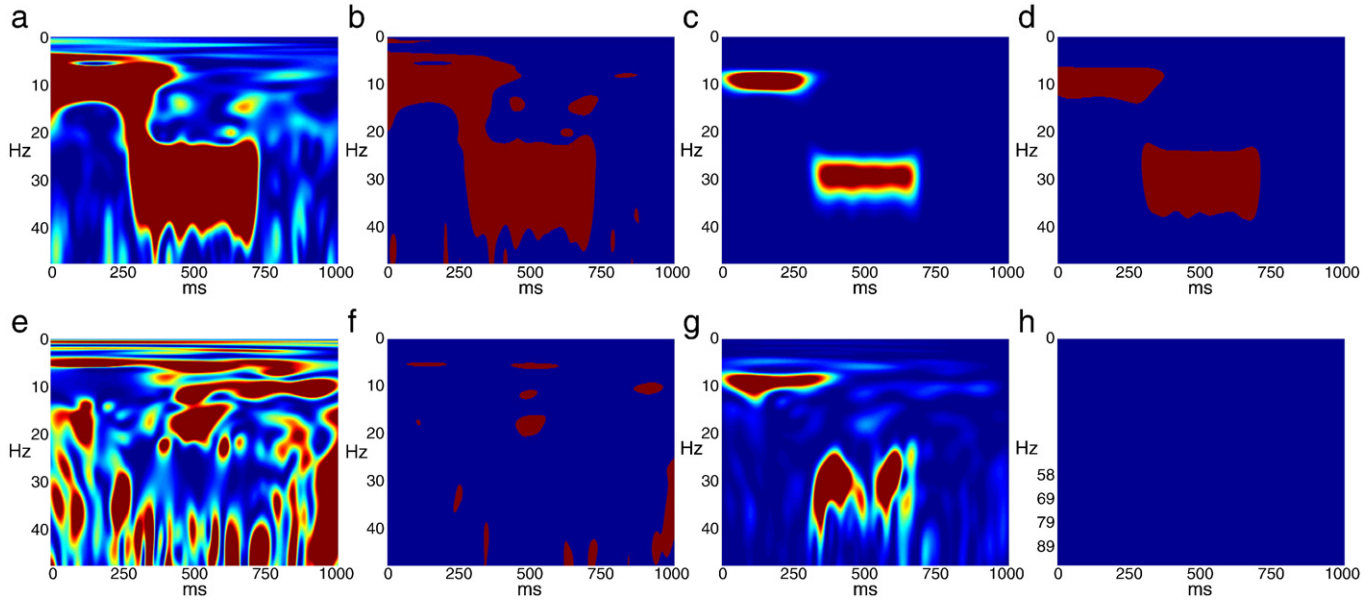

Fig. 5. Example 3—Automatic detection of time–frequency dependence using $n = 30$ trials using either the raw data (first line) or the shuffled data (second line) (a, e) Empirical wavelet coherence $\hat{R}^2_{\mathbf{xy}}(\omega, u)$. (b, f) Significant values (in red) of the empirical wavelet coherence that are above the threshold r_α. (c, g) Empirical WCS $|\hat{S}_{\mathbf{xy}}(\omega, u)|^2$. (d, h) Significant values (in red) of the empirical WCS that are above the threshold $\hat{\lambda}_\alpha$. The value of α is 5% for both thresholds.

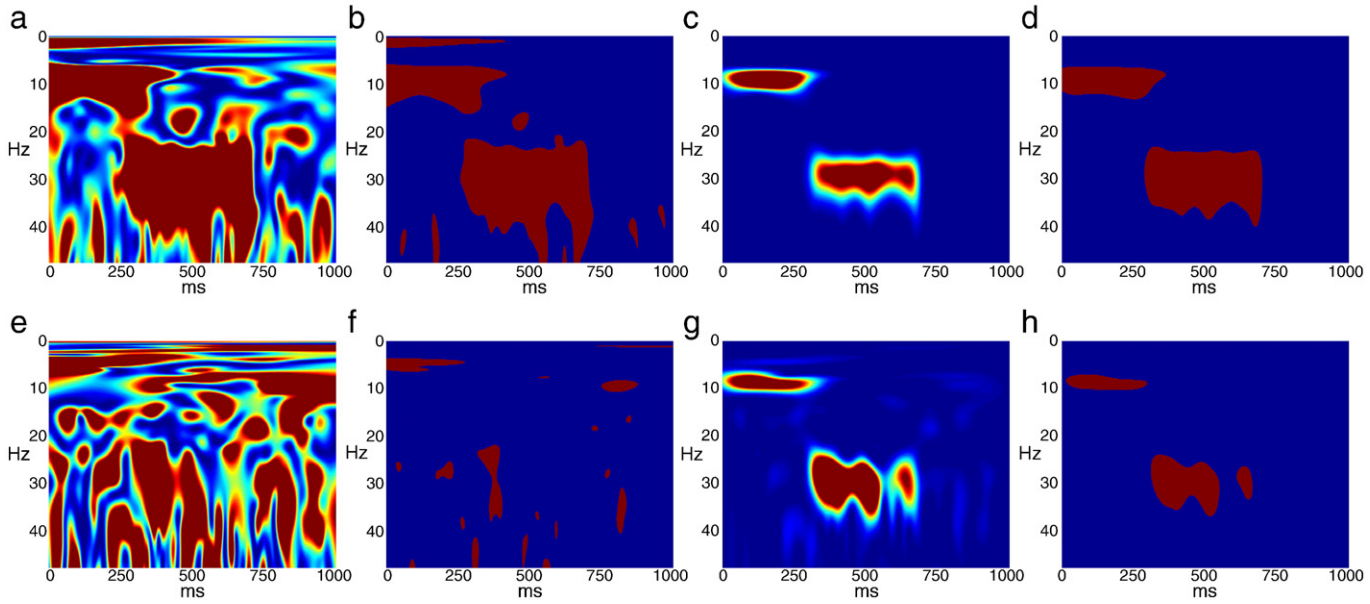

Fig. 6. Example 3—Automatic detection of time–frequency dependence using $n=10$ trials using either the raw data (first line) or the shuffled data (second line) (a, e) Empirical wavelet coherence $\hat{R}^2_{\mathbf{xy}}(\omega,u)$. (b, f) Significant values (in red) of the empirical wavelet coherence that are above the threshold r_α. (c, g) Empirical WCS $|\hat{S}_{\mathbf{xy}}(\omega,u)|^2$. (d, h) Significant values (in red) of the empirical WCS that are above the threshold $\hat{\lambda}_\alpha$. The value of α is 5% for both thresholds.

styloid. The continuous EMG was resampled to 1024 Hz by third-order spline interpolation and high-pass filtered at 3 Hz (zero-lag, 4th order Butterworth filter).

Continuous data were then epoched from −1000 ms to +7000 ms after the onset of the torque feedback, i.e., $T=8192$ for each contraction. After rejection of the trials contaminated by EEG and/or

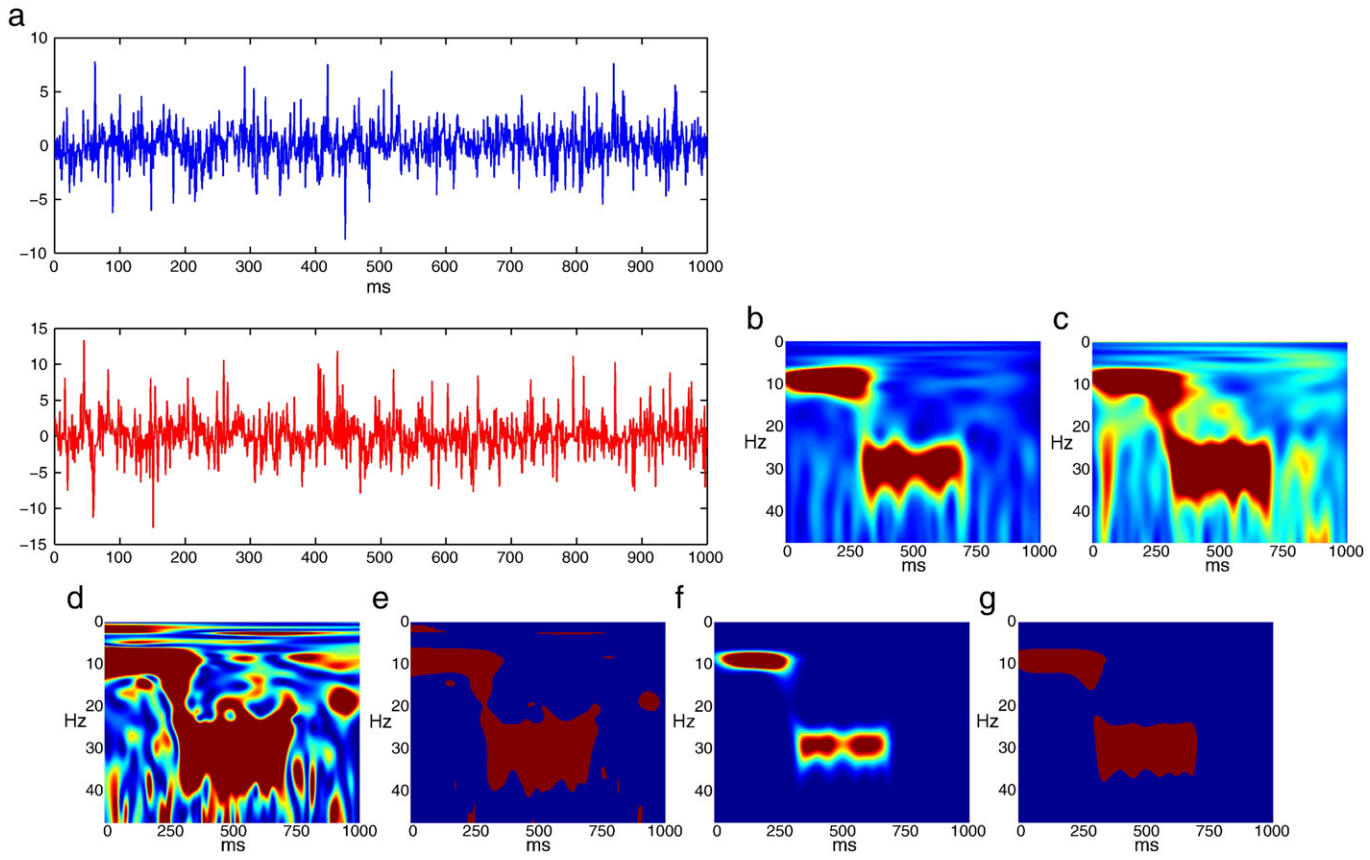

Fig. 7. Example 4—Robustness to Gaussianity using $n=10$ trials with SNR $=-5dB$. (a) An example of time series $\mathbf{x}_1$ and $\mathbf{y}_1$ generated from model (4). (b) Empirical wavelet auto-spectum $\hat{S}_{\mathbf{x}}(\omega,u)$. (c) Empirical wavelet auto-spectum $\hat{S}_{\mathbf{y}}(\omega,u)$. (d) Empirical wavelet coherence $\hat{R}^2_{\mathbf{xy}}(\omega,u)$. (e) Significant values (in red) of the empirical wavelet coherence that are above the threshold r_α. (f) Empirical WCS $|\hat{S}_{\mathbf{xy}}(\omega,u)|^2$. (g) Significant values (in red) of the empirical WCS that are above the threshold $\hat{\lambda}_\alpha$. The value of α is 5% for both thresholds.

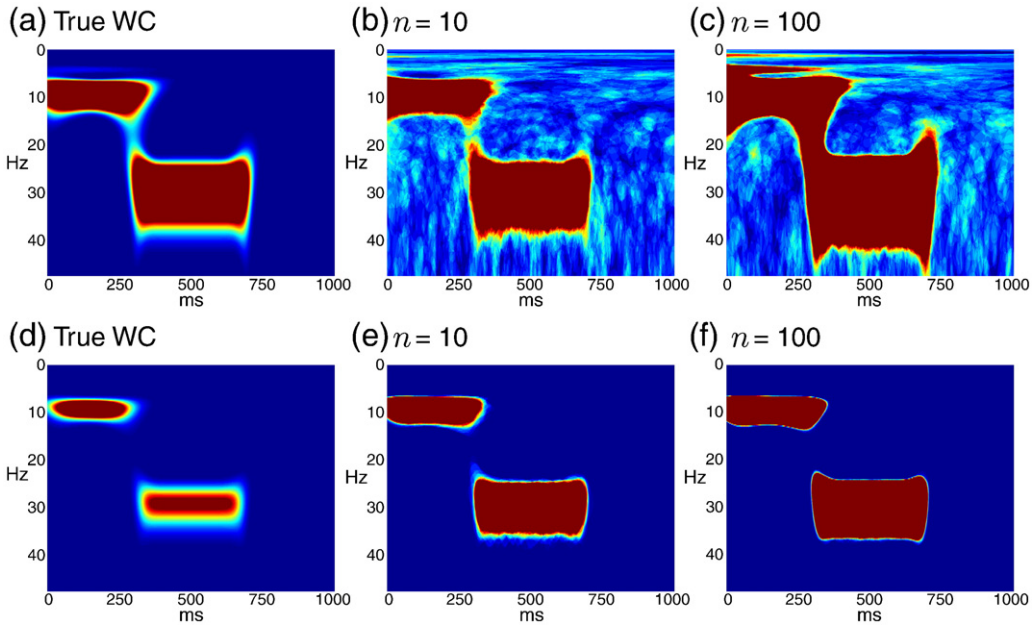

Fig. 8. Simulations with SNR $= -10dB$. (a) True wavelet coherence $R^2_{\mathbf{xy}}(\omega, u)$. (d) True WCS $|S_{\mathbf{xy}}(\omega, u)|^2$. First row: averaged testing map for the detection of significant values of the wavelet coherence with (b) $n = 10$ and (c) $n = 100$. Second row: averaged testing map for the detection of significant values of the WCS with (e) $n = 10$ and (f) $n = 100$ (red indicates values close to 1 and blue indicates values close to 0).

EMG artefacts, the number of remaining contraction was $n = 70$ for each MVC level. Thus, the value of the ratio T/n is in agreement with the conditions discussed in the Appendix in the sense that T is much larger than n.

Experimental results

Fig. 10 (third to fifth row) present the values of the WCS and the wavelet coherence between EEG and EMG, and their corresponding significant values, for a large number of trials ($n = 70$). First, the results show that WCS and wavelet coherence contain different information. Large values of wavelet coherence are widely spread in the time–frequency plane whatever the MVC level, without clear difference in the correlation between EEG and EMG during the rest and contraction periods. To the contrary, large values of WCS are observed for non-null MVC levels in frequency bands centered at 10 Hz and 20 Hz, specifically on the time interval of muscular contraction (knee extension). Secondly, the statistical test using the threshold r_α finds isolated significant values of the wavelet coherence, dispersed both in time and frequency, whatever the MVC level. The

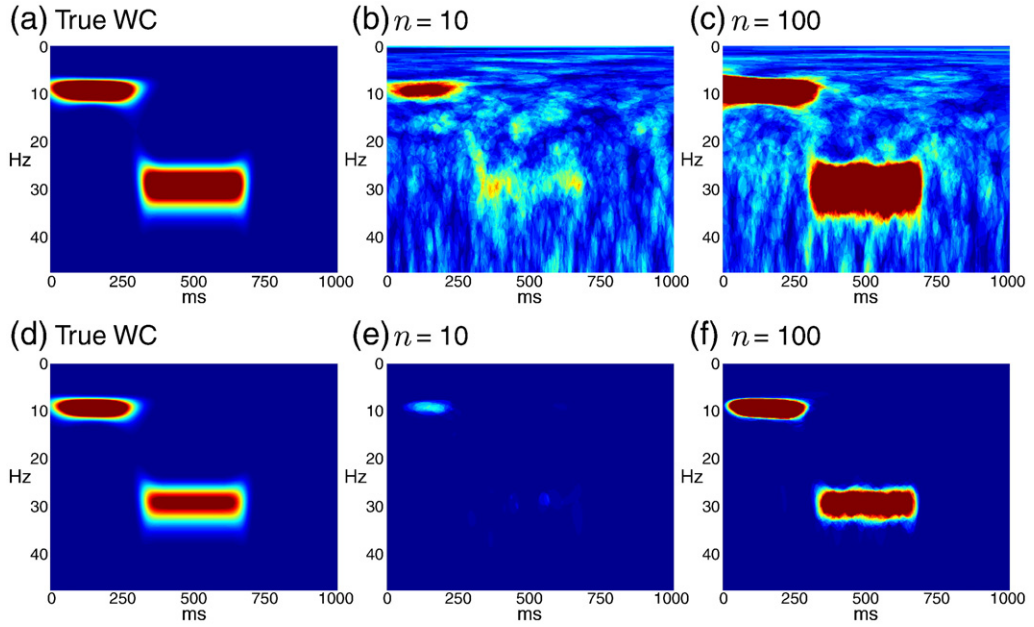

Fig. 9. Simulations with SNR $= -20dB$. (a) True wavelet coherence (WC) $R^2_{\mathbf{xy}}(\omega, u)$. (b) True WCS $|S_{\mathbf{xy}}(\omega, u)|^2$. First row: averaged testing map for the detection of significant values of the wavelet coherence with (b) $n = 10$ and (c) $n = 100$. Second row: averaged testing map for the detection of significant values of the WCS with (e) $n = 10$ and (f) $n = 100$ (red indicates values close to 1 and blue indicates values close to 0).

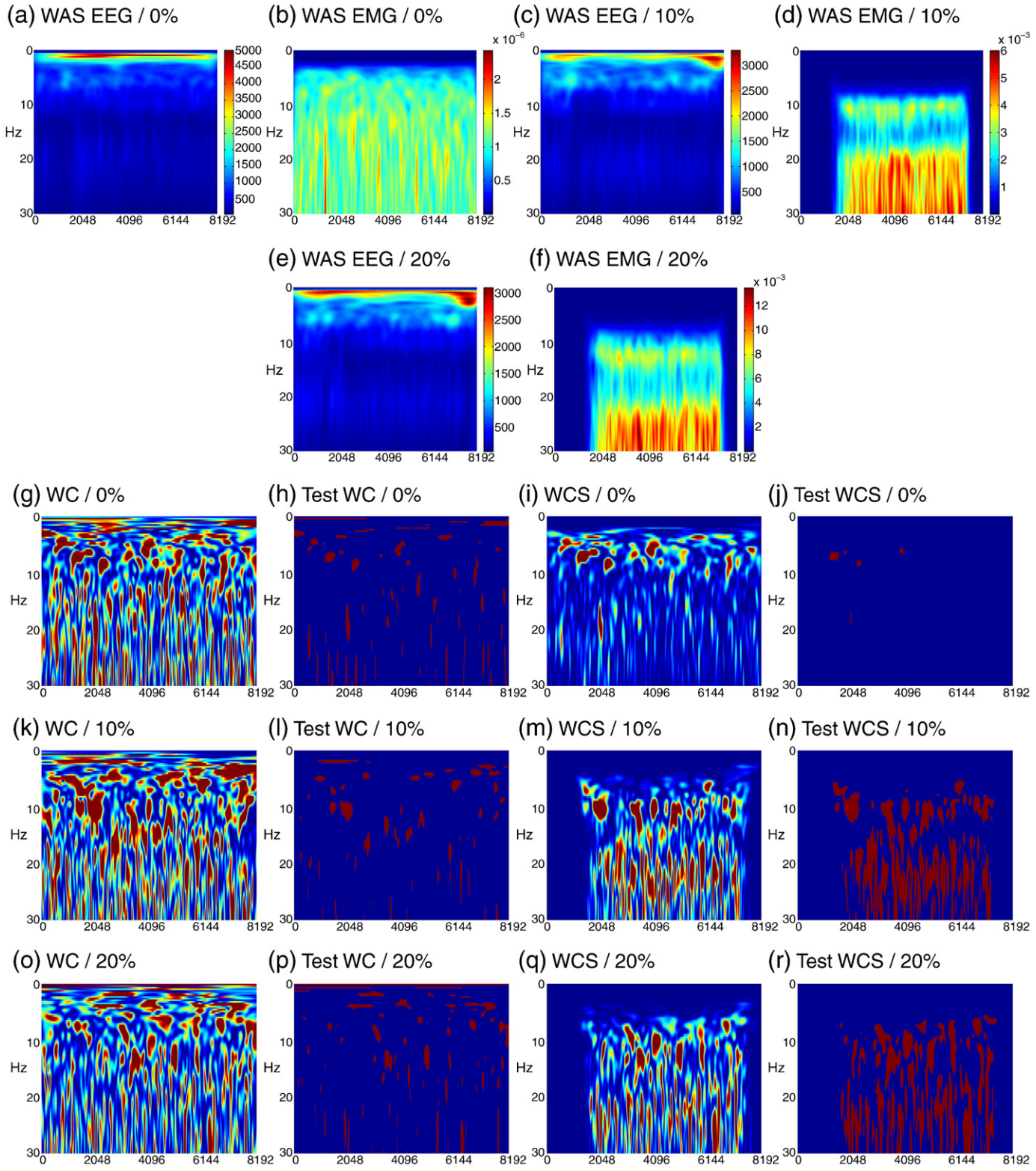

Fig. 10. Analysis of wavelet coherence and WCS on EEG and EMG during isometric contractions of the knee extensors using $n = 70$ trials. First row : empirical wavelet auto-spectra (WAS) of EEG and EMG for MVC = 0%, (no efforts) and MVC = 10%. Second row: WAS of EEG and EMG for MVC = 20%. Third row : data MVC = 0%, (no efforts), fourth row: data for MVC = 10%, fifth row data for MVC = 20%. First column: empirical wavelet coherence $\hat{R}^2_{\mathbf{xy}}(\omega, u)$. Second column: significant values (in red) of the empirical wavelet coherence that are above the threshold r_α. Third column: empirical WCS $|\hat{S}_{\mathbf{xy}}(\omega, u)|^2$. Fourth column: significant values (in red) of the empirical WCS that are above the threshold $\hat{\lambda}_\alpha$.

test detects significant areas in the time–frequency plane during rest periods and does not display a clear correlation between EEG and EMG during maintained knee extension. Opposite to these results, the proposed test using the threshold $\hat{\lambda}_\alpha$ reveals absence of correlation between EEG and EMG during rest periods and for 0% MVC, and finds bands of significant correlation centered at 10 Hz and 20 Hz during knee extension for 10% and 20% MVC. In addition to these highlighted features, the statistical test based on the thresholding of the WCS

indicates clearer differences in the correlation between EEG and EMG with increased MVC level.

Another benefit of our approach is that it gives good results with very few trials. To illustrate this fact, we display the results obtained when using only $n = 10$ trials (randomly chosen from the 70 trials) in Fig. 11. Using a smaller number of trials ($n = 10$, see Fig. 11), similar differences are observed between the WCS and the wavelet coherence, and a similar trend is found between the two tests. Apart from this general result, the significant values of the wavelet coherence (threshold r_α) indicate increased dispersion of the correlation between EEG and EMG in the time–frequency plane with $n = 10$ than with n = 70. When thresholding the WCS with $\hat{\lambda}_\alpha$, it

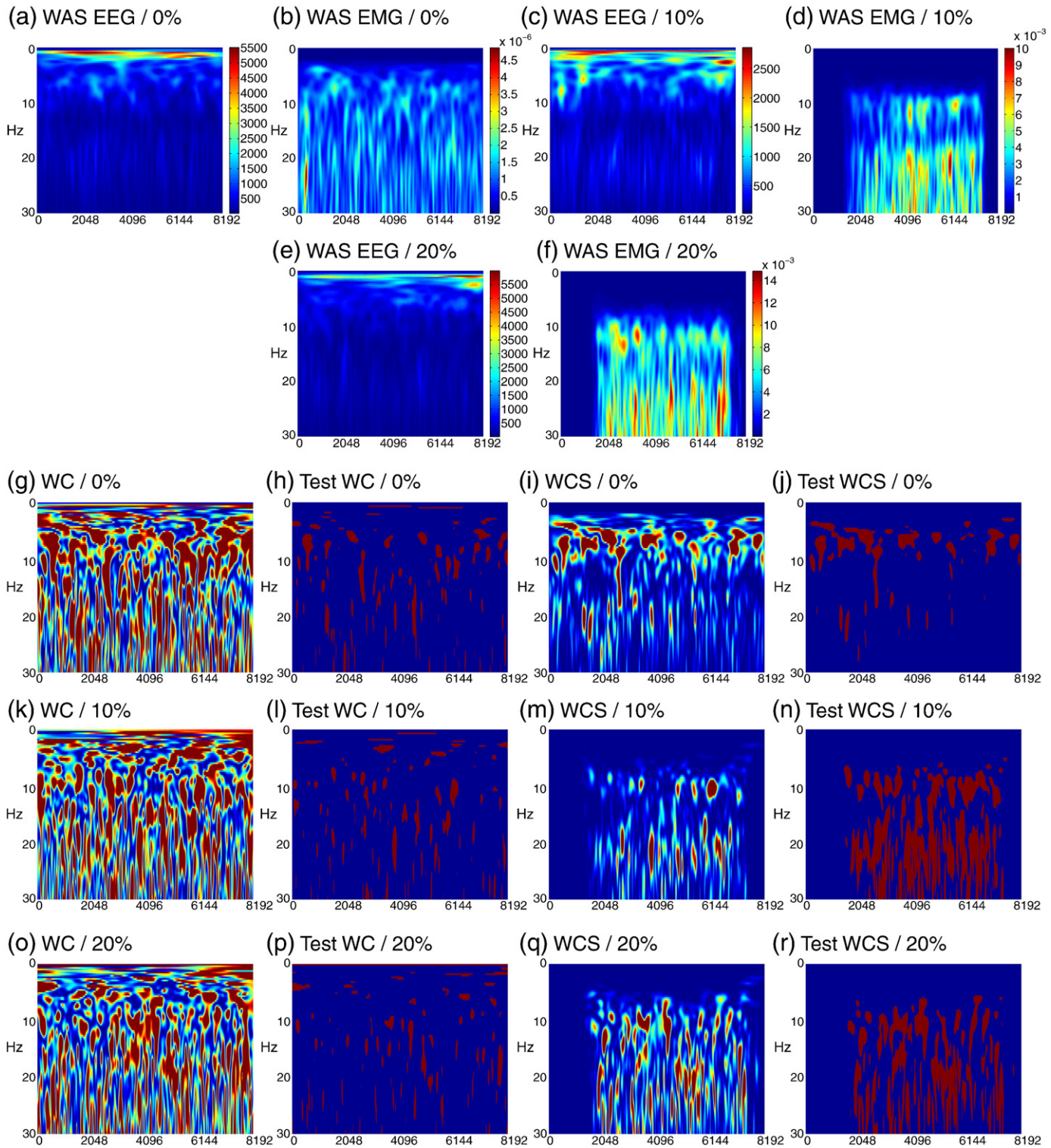

Fig. 11. Analysis of wavelet coherence and WCS on EEG and EMG during isometric contractions of the knee extensors using only $n = 10$ trials. First row : empirical wavelet auto-spectra (WAS) of EEG and EMG for MVC = 0%, (no efforts) and MVC = 10%. Second row: WAS of EEG and EMG for MVC = 20%. Third row : data MVC = 0%, (no efforts), fourth row: data for MVC = 10%, fifth row data for MVC = 20%. First column: empirical wavelet coherence (WC) $\hat{R}^2_{\mathbf{xy}}(\omega, u)$. Second column: significant values (in red) of the empirical wavelet coherence that are above the threshold r_α. Third column: empirical WCS $|\hat{S}_{\mathbf{xy}}(\omega, u)|^2$. Fourth column: significant values (in red) of the empirical WCS that are above the threshold $\hat{\lambda}_\alpha$.

can be seen from Fig. 11(n) and (r) c results i) in broader bands centered at 10 Hz and 20 Hz of significant correlation between EEG and EMG, and ii) in the detection of significant areas centered at 7 Hz during periods of rest, see Fig. 11(j).

Data shuffling

For MVC = 10% and MVC = 20%, Fig. 10(c, e) show large variations of the EEG WAS power specifically in the frequency bands of interest centered at 10 Hz and 20 Hz (i.e., alpha and beta bands, respectively), when compared to the case MVC = 0%, Fig. 10(a). This marked variation in the autospectra causes variation in the WCS, and one may wonder if our test automatically adapts to the change in magnitude of the WCS while still allowing a consistent detection of the significant values of the WCS. To illustrate this point, we used data shuffling as follows. We have compared the results of our test when computing either a WCS using the EEG trials at MVC = 0% and the EMG trials at MVC = 0% or a WCS using the EEG trials at MVC = 20% and the EMG trials at MVC = 0%. In both cases our test detects very few significant values in the WCS (see Fig. 12(d) and compare with Fig. 10(j)).

Discussion

Theoretical comparison of the two statistical procedures

Our method has been analyzed from the point of view of statistical hypothesis testing. With small probability, the procedure rejects the null hypothesis that the repeated trials come from two independent Gaussian time series. The method is thus valid for the analysis of any Gaussian processes with zero mean, in particular for those that are not stationary. Its use is therefore more general than the standard test for significant wavelet coherence detection which is mainly valid for the null hypothesis that the two time series are independent white noise.

Comparison using simulated data

First, if the level of noise in the measurements is high, then the "true" wavelet coherence and the "true" WCS tend to carry the same kind of information on time–frequency dependence between two time series. However, the testing procedures using either the empirical wavelet coherence or the empirical WCS clearly yield to very different conclusions on the nature of the correlations between two times series.

The numerical experiments show that the use of the standard test using wavelet coherence yields erroneous coherence detection (type I error in statistical hypothesis testing), and can miss truly significant values (type II error in statistical hypothesis testing). In particular, this test detects areas the time–frequency plane where no correlation between the signals exists. Indeed, for all values of SNR and numbers of trials, the test using the wavelet coherence yields many false positive, which clearly questions the interpretability of this test and its level of confidence. To the contrary, our procedure correctly estimates the areas in the time–frequency plane where the dependence between the time series is truly significant. Moreover, our test does not detect any area where no correlation between the signals exists, meaning that our test is more conservative.

These results using data shuffling support the argument that our test is adapted to the case where the auto-spectrum of each time series can be very large. Hence, a value of the WCS above the threshold $\hat{\lambda}_\alpha$ can generally be considered as being due to time–frequency dependence between the signals.

With very few trials, the results obtained using the test on wavelet coherence detection are extremely unsatisfactory. To the contrary, our procedure to detect significant values of the cross-spectrum performs very well with few repeated observations. Indeed, the results obtained with only $n = 2$ trials clearly show that our test correctly estimates the areas in the time–frequency plane where the dependence between the time series is truly significant, and does not detect any area where no correlation between the signals exists.

The numerical examples also demonstrate some robustness of the test to the assumption that the time series should be Gaussian.

To the best of our knowledge, this testing procedure to detect significant values of the cross-spectrum is new, and we believe that it represents a powerful alternative to some limitations of wavelet coherence analysis.

Discussion on the analysis of corticomuscular interactions

Our results on the analysis of the correlation between EEG and EMG, i.e. the corticomuscular interactions, emphasize those obtained from simulated data and illustrate the potential of the proposed test to effectively detect time–frequency dependence between non-stationary signals. Thresholding the WCS with the data-based threshold $\hat{\lambda}_\alpha$ overcomes the effects of both time and frequency scaling observed when thresholding the wavelet coherence with r_α. In agreement with previous findings on corticomuscular synchronization (for review, see Mima and Hallett (1999a); Salenius and Hari (2003)), the proposed statistical test improves the detection of the significant areas of correlation at 10 Hz and 20 Hz between EEG and EMG in the time–frequency plane. Significant corticomuscular interactions were found around 20 Hz in agreement with the literature (see Conway et al. (1995); Kilner et al. (2000); Salenius et al. (1997)) but also around 10 Hz, a finding that is less common but nonetheless reported in several studies in healthy subjects (see Feige et al. (2000); Marsden et al. (2001)) and in Parkinson's patients (see (Raethjen et al. (2009)).

Using our method, corticomuscular interaction was not significant during the rest periods and during 0% MVC trials. This feature is clearly an advantage of the proposed test for application to the analysis of

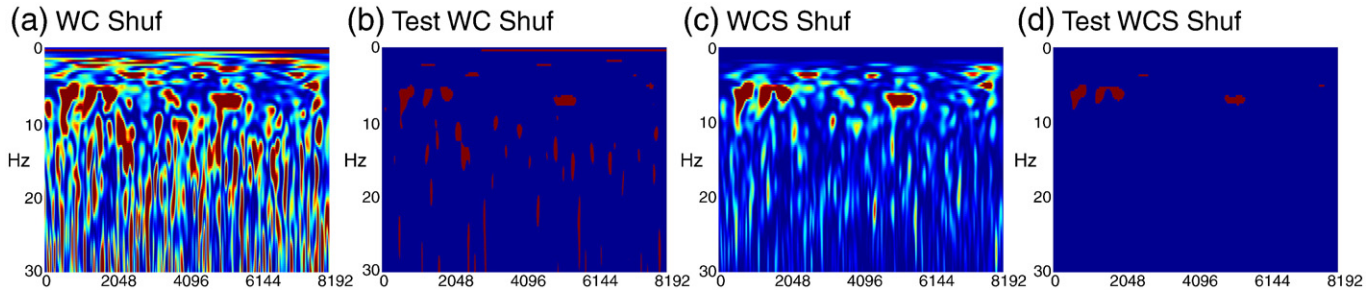

Fig. 12. Analysis of wavelet coherence and WCS on EEG and EMG during isometric contractions of the knee extensors using $n = 70$ trials and data shuffling. First row: data shuffling (EEG − MVC = 20%/EMG − MVC = 0%). First column: empirical wavelet coherence $\hat{R}^2_{\mathbf{xy}}(\omega, u)$. Second column: significant values (in red) of the empirical wavelet coherence that are above the threshold r_α. Third column: empirical WCS $|\hat{S}_{\mathbf{xy}}(\omega, u)|^2$. Fourth column: significant values (in red) of the empirical WCS that are above the threshold $\hat{\lambda}_\alpha$.

corticomuscular interactions, because it does not detect significant area where no correlation exists between the non-stationary signals. For non-null MVC levels, the statistical test on the WCS with $\hat{\lambda}_\alpha$ does not find significant peaks of coherence dispersed in the time–frequency plane. To the contrary, when the number of trials is high ($n=70$), the proposed test detects accurate bands of correlation centered at 10 Hz and 20 Hz during the time interval of muscular contraction. With regards to the results from simulated data, one can suggest that the proposed test estimates more correctly the areas in the time–frequency plane where the dependence between EEG and EMG is truly significant, and that it offers the major advantage to reduce the detection of false positive when compared with the test on the wavelet coherence with r_α.

Another benefit of our approach for application to the analysis of corticomuscular interactions is that the improvement of the detection of corticomuscular interactions is maintained with a small number of trials. Despite an observed increased dispersion in frequency with few trials ($n=10$), the results obtained using the proposed test conserve similar general features to those observed with a large number of trials, which illustrates the practical advantage of our approach when the clinical conditions limit the possible number of experimental trials.

Finally, using data shuffling, we have shown that our method automatically includes an estimation of the variance of the two time series in the computation of the threshold used to detect significant value of the WCS. Indeed, although in the case EEG − MVC = 0%/EMG − MVC = 0% the magnitude of the WCS increases, our test does not detect more significant time–frequency dependence which is consistent with the fact that connectivity does not change when compared to the case EEG − MVC = 20%/EMG − MVC = 0%.

Advantages of WCS in contrast with wavelet coherence

Although the cross-spectrum is a non-normalized measure of dependence, our testing procedure can be used to detect significant values of the empirical WCS since it automatically estimates the amplitude of the auto-spectra of the time series. Coherence is often considered as being more interpretable since it is a normalized measure. However, results in this paper clearly show that a significant value of wavelet coherence (above the detecting threshold r_α) does not necessarily correspond to a significance level of time–frequency dependence. Hence, the use of the standard test on wavelet coherence may lead to erroneous conclusions. To the contrary, in many situations, the use of the WCS combined with our testing procedure is a much more reliable way to detect areas in the time–frequency plane where the dependence between two time series is truly significant. Although we have demonstrated some robustness to Gaussianity, a limitation of our approach is that the derivation of the threshold <mbda$_\alpha$ relies on the assumption that the time series are Gaussian.

Conclusion

We have proposed a new statistical test to detect significant values of the wavelet cross-spectrum between two time series using repeated trials. These values correspond to a truly significant level of time–frequency dependence between the two time series. The test is a fully data-driven procedure based a simple thresholding of the wavelet cross-spectrum. Throughout the paper, this method has been compared with the standard test described in the literature to detect significant values of wavelet coherence between two time series. Comparisons have been made using both theoretical arguments and numerical experiments.

In usual experiments in neuroscience, one often wants to know if a WCS is statistically different from another WCS. This corresponds to the null hypothesis that the difference between two WCS computed from two data sets consisting of pair of time series is zero. A natural procedure to test such an hypothesis would be to compute the difference between two empirical WCS, and then to use an appropriate threshold to detect significant values of the resulting time–frequency map. We believe that the theoretical arguments developed in this paper could be used to derive such a threshold, which represents an interesting topic for future work.

Acknowledgments

This work was supported by the research project grant AO3 NeuroBiomeCo from the University Paul Sabatier. J. Bigot would like to thank the Center for Mathematical Modeling and the CNRS for financial support and excellent hospitality while visiting Santiago where part of this work was carried out. Numerical experiments have been implemented using the MATLAB programming environment and the MATLAB package provided by Aslak Grinsted for performing cross-wavelet and wavelet coherence analysis which can be downloaded at: http://www.pol.ac.uk/home/research/waveletcoherence/.

Appendix

Derivation of the threshold $\hat{\lambda}_\alpha$

The following proposition shows that it is possible to derive under $H_0(\Sigma_x, \Sigma_y)$ a probabilistic upper bound for the empirical WCS (the proof is given in Section 5.2). The key quantities to control such an upper bound are the maximal eigenvalues ρ_x^2 and ρ_y^2 of the covariance matrices Σ_x and Σ_y defined as $\rho_x^2 = max_{v\in\mathbb{R}^T}\frac{v'\Sigma_x v}{v'v}$ and $\rho_y^2 = max_{v\in\mathbb{R}^T}\frac{v'\Sigma_y v}{v'v}$. Note that in the case where $\Sigma_x=\sigma_x^2 I_T$ and $\Sigma_y=\sigma_y^2 I_T$ then $\rho_x^2=\sigma_x^2$ and $\rho_y^2=\sigma_y^2$.

Proposition 5.1. Suppose that the hypothesis $H_0(\Sigma_x, \Sigma_y)$ is true. Let $0<\alpha<1$. Assume that ψ is the Morlet wavelet defined in (2.1). For any frequency ω and time u, define the threshold

$$\lambda_\alpha = \frac{\rho_x\rho_y}{n}\|\psi_{\omega,u}\|^2\left(-log(\alpha/2)+\sqrt{-2nlog(\alpha/2)}\right),$$

where $\|\psi_{\omega,u}\|^2=\sum_{k=1}^{T}|\psi_{\omega,u}(t_k)|^2$ and $\psi_{\omega,u}(t_k)=\sqrt{\frac{\omega}{\omega_0}}\psi\left(\frac{\omega}{\omega_0}(t_k-u)\right)$. Then, for any $n\geq 1$

$$\mathbb{P}\left(|\hat{S}_{\mathbf{xy}}(\omega,u)|>\lambda_\alpha\right)\leq\alpha,$$

where for a random variable Z and a real $t>0$, the notation $\mathbb{P}(|Z|>t)$ denotes the probability of the event that the modulus of Z is greater than t.

In all the numerical experiments of the paper, *the energy (or L^2 norm) of the wavelet ψ is normalized to be one at all scales (meaning that $\|\psi_{\omega,u}\|^2=1$)*. Under such an assumption, the threshold λ_α does not depend on the frequency ω and time u, and one can take the simplified threshold

$$\lambda_\alpha = \frac{\rho_x\rho_y}{n}\left(-log(\alpha/2)+\sqrt{-2nlog(\alpha/2)}\right).$$

Note also that Proposition 5.1 can be applied with any mother wavelet ψ that is a real-valued function. However, this procedure is obviously not directly applicable to real data, as the covariance matrices Σ_x and Σ_y and thus the eigenvalues ρ_x^2 and ρ_y^2 are typically unknown in practice. Nevertheless, data-based values for these parameters can be given. Indeed, if one observes n repeated trials $(\mathbf{x}_m)_{m=1,\ldots,n}$ and $(\mathbf{y}_m)_{m=1,\ldots,n}$ (viewed as n independent realizations of the stochastic processes $\mathbf{x}$ and $\mathbf{y}$ respectively) then one can define

unbiased estimators of Σ_x and Σ_y by taking the following empirical covariance matrices

$$\hat{\Sigma}_x = \frac{1}{n}\sum_{m=1}^{n} \mathbf{x}_m \mathbf{x}_m' \text{ and } \hat{\Sigma}_y = \frac{1}{n}\sum_{m=1}^{n} \mathbf{y}_m \mathbf{y}_m'.$$

It is then tempting to estimate ρ_x^2 and ρ_y^2 by the maximal eigenvalues $\hat{\rho}_x^2$ and $\hat{\rho}_y^2$ of the empirical covariance matrices $\hat{\Sigma}_x$ and $\hat{\Sigma}_y$ defined as

$$\hat{\rho}_x^2 = \max_{v\in\mathbb{R}^T} \frac{v'\hat{\Sigma}_x v}{v'v} \text{ and } \hat{\rho}_y^2 = \max_{v\in\mathbb{R}^T} \frac{v'\hat{\Sigma}_y v}{v'v}.$$

Note that the quantities $\hat{\rho}_x^2$ and $\hat{\rho}_y^2$ are not difficult to compute numerically using standard software such as the MATLAB programming environment. However, results from random matrix theory (see El Karoui (2007) and references therein) show that $\hat{\rho}_x^2$ and $\hat{\rho}_y^2$ are not consistent estimators of ρ_x^2 and ρ_y^2. Indeed, in the case where $\Sigma_x = \sigma_x^2 I_T$ and $\Sigma_y = \sigma_y^2 I_T$ then

$$\lim_{n\to+\infty, T\to+\infty} \hat{\rho}_x = \sigma_x(1+\sqrt{\gamma}) \text{ and } \lim_{n\to+\infty, T\to+\infty} \hat{\rho}_y = \sigma_y(1+\sqrt{\gamma})$$

where $\gamma = \lim_{n\to+\infty, T\to+\infty} \frac{T}{n}$. Therefore if $\gamma>0$ then $\hat{\rho}_x$ does not converge to σ_x. The coefficient γ reflects the ratio between the length T of the time series and the number of trials n. Typically, T is much larger than n and in practice, the ratio $\frac{T}{n}$ can be larger than 10 or 100, meaning that the ratio $\frac{\hat{\rho}_x}{\sigma_x} \approx (1+\sqrt{\gamma})$ is not close to one. This phenomena is a well known problem for the statistical estimation of large covariance matrices (see e.g. Bickel and Levina (2008) and references therein) in the high-dimensional data setting when the size of the data (here the number of time points T) is much larger than the number of repeated observations n.

In the more general case where $\Sigma_x \neq \sigma_x^2 I_T$ or $\Sigma_y \neq \sigma_y^2 I_T$, using Theorem II.13 in Davidson and Szarek (2001) it can be shown that for any value of $0<\beta\leq 1$ and any fixed $n\geq 1$ and $T\geq 1$ then

$$\mathbb{P}\left(\hat{\rho}_x \geq \rho_x\left(1+\sqrt{\frac{T}{n}}+\sqrt{\frac{-2\log(\beta)}{n}}\right)\right)\leq\beta.$$

These results therefore suggest to estimate ρ_x and ρ_y by $\hat{\rho}_x \Big/ \left(1+\sqrt{\frac{T}{n}}\right)$ and $\hat{\rho}_y \Big/ \left(1+\sqrt{\frac{T}{n}}\right)$ which leads to the use of the following data-based threshold $\hat{\lambda}_\alpha$ (in the case where the energy of the wavelet ψ is normalized to be one)

$$\hat{\lambda}_\alpha = \frac{\hat{\rho}_x\hat{\rho}_y}{\left(1+\sqrt{\frac{T}{n}}\right)^2}\left(-\frac{\log(\alpha/2)}{n}+\sqrt{-\frac{2\log(\alpha/2)}{n}}\right).$$

Proof of Proposition 5.1

Let $Z = \hat{S}_{\mathbf{xy}}(\omega,u)$ and remark that under H_0 the random variable Z can be written as

$$Z = \frac{1}{n}\sum_{m=1}^{n} X_{m,1}'\Sigma_x^{1/2}a\overline{a'}\Sigma_y^{1/2}X_{m,2},$$

where $X_{m,1}$ and $X_{m,2}$ are independent centered Gaussian vector in $\mathbb{R}^T$ with covariance matrix the identity, and a is the deterministic vector in $\mathbb{C}^T$ with entries

$$a = \left[\psi_{\omega,u}(t_k)\right]_{k=1}^{T} \text{ where } \psi_{\omega,u}(t_k) = \sqrt{\frac{\omega}{\omega_0}}\psi\left(\frac{\omega}{\omega_0}(t_k-u)\right).$$

Then, define the following vector $X\in\mathbb{R}^{n2T}$ by concatenation of the vectors $X_{m,1}$ and $X_{m,2}$ in the following way:

$$X = \begin{pmatrix} X_{m,1} \\ X_{m,2}\end{pmatrix}_{m=1,\dots,n} \in\mathbb{R}^{n2T}.$$

Note that X is a centered Gaussian vector with covariance matrix the identity. Then, define the $2T\times 2T$ matrix with complex entries

$$A_{xy} = \frac{1}{2n}\begin{pmatrix}\Sigma_x^{1/2} & 0\\ 0 & \Sigma_x^{1/2}\end{pmatrix}\begin{pmatrix}0 & a\overline{a'}\\ \overline{a}a' & 0\end{pmatrix}\begin{pmatrix}\Sigma_y^{1/2} & 0\\ 0 & \Sigma_y^{1/2}\end{pmatrix}$$

and introduce the following $n2T\times n2T$ block-diagonal matrix

$$A = \begin{pmatrix} A_{xy} & 0 & \dots & 0\\ 0 & A_{xy} & 0 & 0\\ \vdots & 0 & \dots & 0\\ 0 & 0 & 0 & A_{xy}\end{pmatrix}.$$

Given the definition (2.1) of the Morlet wavelet ψ, one can check that the matrix $a\overline{a'}$ is Hermitian which implies that the matrices A_{xy} and A are Hermitian. Then, one can remark that the random variable mphZ can be written in the form of a χ^2 variable as

$$Z = X'AX.$$

Now, the result of Proposition 5.1 follows from the lemma below (its proof follows from standard arguments on the concentration of χ^2 variables, see e.g. Proposition 3 in Comte (2001) and Lemma 1 in Laurent and Massart (2000)):

Lemma 5.2. Let $X\in\mathbb{R}^p$ be a centered Gaussian vector with covariance matrix the identity. Let Γ be a $p\times p$ Hermitian matrix (with complex entries). Let $\gamma_1, \dots, \gamma_p$ be the eigenvalues of Γ. Define

$$\gamma = \max_{1\leq i\leq p}\{|\gamma_i|\} \text{ and } s^2 = \sum_{i=1}^{p}|\gamma_i|^2.$$

Then, for any $\eta>0$ one has that

$$\mathbb{P}\left(|X'\Gamma X - tr(\Gamma)|\geq 2\gamma\eta + 2\sqrt{s^2\eta}\right)\leq 2\exp(-\eta),$$

where $tr(\Gamma)$ is the trace of the matrix Γ.

Then, remark that the eigenvalues of the $2T\times 2T$ Hermitian matrix A_{xy} are smallest than $\frac{\rho_x\rho_y}{2n}\|a\|^2$, where $\|z\|$ denotes the standard Euclidean norm of a vector z in C^T. Therefore, if one denotes by $\gamma_1, \dots, \gamma_p$ the eigenvalues of A with $p=2nT$, it follows that

$$\max_{1\leq i\leq p}\{|\gamma_i|\}\leq\frac{\rho_x\rho_y}{2n}\|a\|^2.$$

Remark also that A_{xy}^2 is of rank 2 with eigenvalues bounded by $\left(\frac{\rho_x\rho_y}{2n}\|a\|^2\right)^2$ and therefore

$$\sum_{i=1}^{p}|\gamma_i|^2 = tr\left(A^2\right) = ntr\left(A_{xy}^2\right)\leq 2n\left(\frac{\rho_x\rho_y}{2n}\|a\|^2\right)^2 = \frac{\rho_x^2\rho_y^2}{2n}\|a\|^4.$$

Finally, note that

$$\|a\|^2 = \|\psi_{\omega,u}\|^2 \text{ where } \|\psi_{\omega,u}\|^2 = \sum_{k=1}^{T}|\psi_{\omega,u}(t_k)|^2.$$

Therefore, using that $tr(A)=0$ and by applying Lemma 5.2 with $p=2nT, \Gamma=A, \gamma=\frac{1}{2n}\rho_x\rho_y\|\psi_{\omega,u}\|^2$ and $s^2=\frac{1}{2n}\rho_x^2\rho_y^2\|\psi_{\omega,u}\|^4$, it follows that for any $\eta>0$

$$\mathbb{P}\left(|Z|\geq\frac{\rho_x\rho_y}{n}\|\psi_{\omega,u}\|^2\left(\eta+\sqrt{2n\eta}\right)\right)\leq 2exp(-\eta).$$

Thus, the result of Proposition 5.1 follows by taking $\eta=-log(\alpha/2)$ which completes the proof. □

References

Allen, D., MacKinnon, C.D., 2010. Time–frequency analysis of movement-related spectral power in eeg during repetitive movements: a comparison of methods. J. Neurosci. Meth. 186, 107–115.

Bickel, P., Levina, E., 2008. Covariance regularization by thresholding. Ann. Stat. 36, 2577–2604.

Buzsaki, G., Draguhn, A., 2004. Neuronal oscillations in cortical networks. Science 304, 1926–1929.

Comte, F., 2001. Adaptative estimation of the spectrum of a stationary gaussian sequence. Bernoulli 7, 267–298.

Conway, B., Halliday, D., Farmer, S., Shahani, U., Maas, P., Weir, A.I., et al., 1995. Synchronization between motor cortex and spinal motoneuronal pool during the performance of a maintained motor task in man. J. Physiol. 489, 917–924.

Davidson, K.R., Szarek, S.J., 2001. Local operator theory, random matrices and Banach spaces. Handbook of the geometry of Banach spaces, Vol. I. North-Holland, Amsterdam, pp. 317–366.

El Karoui, N., 2007. Tracy–Widom limit for the largest eigenvalue of a large class of complex sample covariance matrices. Ann. Probab. 35, 663–714.

Feige, B., Aertsen, A., Kristeva-Feige, R., 2000. Dynamic synchronization between multiple cortical motor areas and muscle activity in phasic voluntary movements. J. Neurophysiol. 84, 2622–2629.

Gish, H., Cochran, D., 1988. Generalized coherence. International Conference on Acoustics, Speech, and Signal Processing, pp. 2745–2748.

Grinsted, A., Moore, J.C., Jevrejeva, S., 2004. Application of the cross wavelet transform and wavelet coherence to geophysical time series. Nonlinear Processes Geophys. 11, 561–566.

Grosse, P., Cassidy, M., Brown, P., 2002. Eeg–emg, meg–emg and emg–emg frequency analysis: physiological principles and clinical applications. Clin. Neurophysiol. 113, 1523–1531.

Gurley, G., Kijewski, T., Kareem, A., 2003. First- and higher-order correlation detection using wavelet transforms. J. Neurosci. Meth. 129, 188–201.

Halliday, D., Conway, B., Farmer, S., Rosenberg, J., 1998. Using electroencephalography to study functional coupling between cortical activity and electromyograms during voluntary contractions in humans. Neurosci. Lett. 241, 5–8.

Halliday, D.M., Rosenberg, J.R., Amjad, A.M., Breeze, P., Conway, B.A., Farmer, S.F., 1995. A framework for the analysis of mixed time series/point process data—theory and application to the study of physiological tremor, single motor unit discharges and electromyograms. Progr. Biophys. Mol. Biol. 64, 237–278.

Hermens, H., Freriks, B., Disselhorst-Klug, C., Rau, G., 2000. Development of recommendations for semg sensors and sensor placement procedures. J. Electromyogr. Kinesiol. 10, 361–374.

Kilner, J., Baker, S., Salenius, S., Hari, R., Lemon, R., 2000. Human cortical muscle coherence is directly related to specific motor parameters. J. Neurosci. 20, 8838–8845.

Lachaux, J.P., Lutz, A., Rudrauf, D., Cosmelli, D., Le Van Quyen, M., Martinerie, J., Varela, F., 2002. Estimating the time-course of coherence between single-trial brain signals: an introduction to wavelet coherence. Neurophysiol. Clin. 32, 157–174.

Laurent, B., Massart, P., 2000. Adaptive estimation of a quadratic functional by model selection. Ann. Stat. 28, 1302–1338.

Mallat, S., 1998. A Wavelet Tour of Signal Processing. Academic Press, New York.

Maraun, D., Kurths, J., 2004. Cross wavelet analysis: significance testing and pitfalls. Nonlinear Processes Geophys. 11, 505–514.

Maris, E., Schoffelen, J.M., Fries, P., 2007. Nonparametric statistical testing of coherence differences. J. Neurosci. Meth. 163, 161–175.

Marsden, J., Brown, P., Salenius, S., 2001. Involvement of the sensorimotor cortex in physiological force and action tremor. NeuroReport 12, 1937–1941.

Masakado, Y., Nielsen, J., 2008. Task-and phase-related changes in cortico-muscular coherence. Keio J. Med. 57, 50–56.

Mima, T., Hallett, M., 1999a. Corticomuscular coherence: a review. J. Clin. Neurophysiol. 16, 501–511.

Mima, T., Hallett, M., 1999b. Electroencephalographic analysis of cortico-muscular coherence: reference effect, conduction and generator. Clin. Neurophysiol. 110, 1892–1899.

Mima, T., Steger, J., Gerlo, C., Hallett, M., 2000. Electroencephalographic measurement of motor cortex control of muscle activity in humans. Clin. Neurophysiol. 111, 326–337.

Ombao, H.C., Raz, J.A., von Sachs, R., Malow, B.A., 2001. Automatic statistical analysis of bivariate nonstationary time series. J. Am. Stat. Assoc. 96, 543–560.

Ombao, H., Van Bellegem, S., 2008. Evolutionary coherence of nonstationary signals. IEEE Trans. Signal Process. 56, 2259–2266.

Perez, M., Lundbye-Jensen, J., Nielsen, J., 2006. Changes in corticospinal drive to spinal motoneurones following visuo-motor skill learning in humans. J. Physiol. 573, 843–855.

Raethjen, J., Govindan, R., Muthuraman, M., Kopper, F., Volkmann, J., Deuschl, G., 2009. Cortical correlates of the basic and first harmonic frequency of parkinsonian tremor. Clin. Neurophysiol. 120, 1866–1872.

Salenius, S., Hari, R., 2003. Synchronous cortical oscillatory activity during motor action. Curr. Opin. Neurobiol. 13, 678–684.

Salenius, S., Portin, K., Kajola, M., Salmelin, R., Hari, R., 1997. Cortical control of human motoneuron firing during isometric contraction. J. Neurophysiol. 77, 3401–3405.

Sanderson, J., Fryzlewicz, P., Jones, M.W., 2010. Estimating linear dependence between nonstationary time series using the locally stationary wavelet model. Biometrika 97, 435–446.

Schnitzler, A., Gross, J., 2005. Normal and pathological oscillatory communication in the brain. Nat. Rev. Neurosci. 6, 285–296.

Tallon-Baudry, C., Bertrand, O., Delpuech, C., Pernier, J., 1996. Stimulus specificity of phase-locked and non-phase-locked 40*hz* visual responses in human. J. Neurosci. 16, 4240–4249.

Varela, F., Lachaux, J.P., Rodriguez, E., Martinerie, J., 2001. The brainweb: phase synchronization and large-scale integration. Nat. Rev. Neurosci. 2, 229–239.

Whitcher, B., 2000. Wavelet analysis of covariance with application to atmospheric time series. J. Geophys. Res. 105, 200.

Whitcher, B., Craigmile, P.F., Brown, P., 2005. Time-varying spectral analysis in neurophysiological time series using hilbert wavelet pairs. Signal Process. 85, 2065–2081.

Zhan, Y., Halliday, D., Jiang, P., Liu, X., Feng, J., 2006. Detecting the time-dependent coherence between non-stationary electrophysiological signals—a combined statistical and time–frequency approach. J. Neurosci. Meth. 156, 322–332.